On-Shell Methods for Tree-Level Amplitudes in (De)Constructed Gauge Theory

Author:
Su Yingze

Affiliation:
Theoretical Elementary Particle Physics Laboratory
Department of Physics, Faculty of Science
Nagoya University

Major:
Theoretical Physics

Degree:
Master of Science

Submitted on:
June 2025

Abstract

Name: Su Yingze

Student number: 262309017

This thesis explores tree-level scattering amplitudes in (De)constructed gauge theories using modern on-shell methods. Traditional Feynman diagram techniques, though systematic, become increasingly cumbersome in theories with gauge redundancies and high multiplicity. Motivated by these limitations, we adopt a framework based on analyticity, factorization, and gauge invariance, applying the BCFW recursion relation and related spinor-helicity techniques.

Our analysis focuses on the two-site model, the simplest (De)constructed scenario, which provides a renormalizable four-dimensional realization of dimensional deconstruction and naturally generates Kaluza-Klein (KK)-like spectra. Tree-level color-ordered amplitudes involving massive and massless vector bosons are computed using the BCFW recursion, revealing significant simplifications and cancellation patterns, especially in longitudinal gauge boson scattering. To access non-MHV sectors, we further employ the Cachazo-Svrček-Witten (CSW) expansion, which efficiently constructs NMHV amplitudes from MHV vertices, offering a complementary perspective to BCFW recursion.

Our results demonstrate that on-shell methods remain powerful even in semi-realistic settings with broken gauge symmetry and massive states. The structural simplicity of the resulting amplitudes suggests potential geometric interpretations and invites extensions to loop-level processes.

Future directions include applying generalized unitarity and BCFW-based recursion at loop level, incorporating double-copy constructions to study gravitational analogues, and exploring formulations via the CHY formalism, scattering forms, or positive geometry such as the amplituhedron. These approaches promise deeper insight into the unifying principles behind quantum field theories and the emergence of higher-dimensional behavior from four-dimensional dynamics.

Keywords: scattering amplitudes, on-shell methods, BCFW recursion, (De)constructed gauge theory

Contents

1 Introduction

As we have known, under the conventional quantum field theory framework, Richard Feynman introduced an elegant method—Feynman diagrams—to perturbatively compute scattering amplitudes through diagrammatic expansions. Despite their intuitive and systematic nature, these diagrams quickly become complicated as the complexity of physical theories grows, particularly in gauge theories. When dealing with non-Abelian gauge fields such as gluons, an enormous number of redundant gauge degrees of freedom often arises, significantly increasing computational complexity. This redundancy requires meticulous handling to ensure correct and gauge-invariant results. Furthermore, traditional Feynman diagrams obscure underlying symmetries, such as the dual superconformal symmetry observed explicitly in N = 4 super Yang-Mills theory, making it difficult to identify and exploit these hidden structures.

These challenges have strongly motivated physicists to develop alternative, more efficient methods. Among these, the BCFW recursion relation represents a pivotal breakthrough. Originating from the work of Britto, Cachazo, and Feng, and later generalized in collaboration with Edward Witten, the BCFW recursion provides a powerful method to compute amplitudes by analytically continuing external momenta into the complex plane. By deforming two external momenta with a complex parameter, while maintaining momentum conservation and on-shell conditions, the amplitudes exhibit simplified pole structures, enabling recursive computation from lower-point amplitudes. This method not only streamlines calculations but also naturally reveals hidden symmetries and analytic properties that are invisible through traditional approaches.

Motivated by insights from dimensional deconstruction, this thesis investigates a simplified yet rich class of gauge theories—the (De)constructed gauge theories—where higher-dimensional theories emerge dynamically from four-dimensional renormalizable setups. Proposed initially by Arkani-Hamed, Cohen, and Georgi, these models discretize additional spatial dimensions into gauge groups linked by scalar fields. Specifically, we focus on the simplest example, the two-site model, which dynamically generates Kaluza-Klein-like states. One intriguing phenomenon in these models is the subtle cancellation of amplitudes involving longitudinal modes of massive gauge bosons, which mimics the behavior observed in genuine higher-dimensional gauge theories.

In this work, we apply modern amplitude techniques, such as the BCFW recursion relation and the spinor-helicity formalism, to compute tree-level amplitudes within this two-site framework. By exploring both maximally helicity violating (MHV) and next-to-MHV (NMHV) configurations using the Cachazo-Svrček-Witten (CSW) expansion, we demonstrate significant simplifications and uncover intricate cancellation patterns. These results not only validate the effectiveness of modern on-shell methods in theories with massive and massless gauge fields but also suggest deeper geometric interpretations.

This thesis serves as the foundational step in my research journey, equipping me with essen-

tial knowledge and skills and broadening my perspective in scattering amplitude computations. Through this initial exploration of (De)constructed gauge theories using modern on-shell methods, I have established a robust understanding of tree-level amplitudes and gained familiarity with pivotal tools like the BCFW recursion relation and the spinor-helicity formalism. This groundwork will enable me to efficiently transition into further research directions, facilitating deeper inquiries into various topics in theoretical physics.

The structure of this thesis is organized as follows: Chapter 2 provides a comprehensive review of essential theoretical background, including the color structure of gauge theory and modern amplitude techniques such as BCFW recursion, spinor-helicity formalism, and CSW expansions. Chapter 3 introduces the general (De)constructed gauge theory framework, discussing the overall structure and fundamental concepts relevant to the model. Chapter 4 focuses specifically on detailed computations within the two-site (De)constructed gauge model, presenting thorough analyses of tree-level scattering amplitudes, significant simplifications, and cancellation phenomena. Finally, Chapter 5 summarizes key findings, emphasizing their implications and potential applications, while also identifying future research opportunities inspired by this work.

2 Review of BCFW recursion relation and others

Traditionally, one relies on Feynman diagrams to calculate scattering amplitudes. Feynman diagrams provide a clear picture of physics and a systematic procedure of calculations. They are in textbooks and widely used. But Feynman diagrams are not efficient in complicated calculations for high energy physics. Increasing the number of particles in a scattering, the number of Feynman diagrams increase exponentially. If gauge fields are involved, one easily encounters thousands of diagrams. For example, for pure gluon case, the number of Feynman diagrams for n-gluons at tree-level is given by

n=	4	5	6	7	8	9	10
	4	25	220	2485	34300	559405	10525900

(These numbers are counted with the inclusion of 4 point interaction.)

Not only with huge number of diagrams, the expression for a single Feynman diagram can also be very complicated. For example, the three-graviton vertex has almost 100 terms. It is almost impossible to calculate scattering amplitudes of gravitons directly from Feynman diagrams. For gauge theories, single Feynman diagram usually depends on the gauge. Many terms cancel with each other at the end of process of calculation. In practice, one does not even know where to start most times.

BCFW are devised to solve some of these problems. So in the following part, I will give a systematic introduction to BCFW recursion relation and other necessary tools. This section is mainly based on the excellent review by Elvang and Huang [1].

2.1 Spinor-Helicity Formalisim for Massless Particles

2.1.1 Brief introduction of spinor-helicity formalism

The spinor-helicity formalism just told us that a light-like Lorentz 4-vector can be decomposed to the product of two Weyl spinor. It is quite natural to see it from the representation of Lorentz group. A Lorentz 4-vector lives in $(\frac{1}{2},\frac{1}{2})$ representation, which can be decomposed to $(\frac{1}{2},0)\bigoplus(0,\frac{1}{2})$. We have known that the $(\frac{1}{2},0)$ and $(0,\frac{1}{2})$ correspond to left handed Weyl spinor and right handed Weyl spinor respectively.

Given a null momentum p_μ in four dimension spacetime, we can define a 2×2 matrix by sigma matrix

$$p_{\alpha\dot{\alpha}} = p_\mu \sigma^\mu = \begin{pmatrix} p^0 - p^3 & -p^1 + ip^2 \\ -p^1 - ip^2 & p^0 + p^3 \end{pmatrix}$$

note that $\det p_{\alpha\dot{\alpha}} = 0$ for massless particles, so it is always possible find two Weyl spinor(two components quantity) satsfying the following equation

$$p_\mu \sigma^\mu = p_{\alpha\dot{\alpha}} = \lambda_\alpha \tilde{\lambda}_{\dot{\alpha}} = |\lambda\rangle[\lambda| \tag{2.1}$$

and similarly we can obtain define

$$p_\mu \bar{\sigma}^\mu = p^{\dot{\alpha}\alpha} = \tilde{\lambda}^{\dot{\alpha}} \lambda^\alpha = |\lambda]\langle\lambda|, \tag{2.2}$$

For general complex momenta, the λ_α and $\tilde{\lambda}_{\dot{\alpha}}$ are independent two dimensional complex vectors. For real momenta, the matrix is Hermitian and so we have $\tilde{\lambda}_{\dot{\alpha}} = (\pm)(\lambda_\alpha)^*$.

Thet satisfy the following Weyl equation

$$p_{\alpha\dot{\alpha}}|p]^{\dot{\alpha}} = 0, \quad [p|_{\dot{\alpha}} p^{\dot{\alpha}\alpha} = 0, \quad p^{\dot{\alpha}\alpha}|p\rangle_\alpha, \quad \langle p|^\alpha p_{\alpha\dot{\alpha}} = 0 \tag{2.3}$$

and we can use two-dimension antisymmetric tensor to raise or lower the indices

$$[p|_{\dot{\alpha}} = \varepsilon_{\dot{\alpha}\dot{\beta}}|p]^{\dot{\beta}}, \qquad \langle p|^\alpha = \varepsilon^{\alpha\beta}|p\rangle_\beta \tag{2.4}$$

Then,

The angle and square spinors are the core of **spinor-helicity formalism**.

Here, it is also necessary to introduce the **angle spinor bracket** $\langle pq\rangle$ and **square spinor bracket** $[pq]$, it is the key ingredient for writing amplitudes in terms of spinor-helicity variable.

$$\langle pq\rangle = \langle p|^\alpha |q\rangle_\alpha, \qquad [pq] = [p|_{\dot{\alpha}}|q]^{\dot{\alpha}}. \tag{2.5}$$

Since the indices are raised and lowed by antisymmetric tensor, so the brackets are antisym-

metric:

$$\langle pq\rangle = -\langle qp\rangle, \qquad [pq] = -[qp]. \tag{2.6}$$

There are no $\langle pq]$ brackets, because the indices cannot contract with each other to form a Lorentz scalar.

It is very easy to derive the following important relation:

$$\langle pq\rangle[pq] = 2p \cdot q = (p+q)^2 \tag{2.7}$$

by using (2.1) and

$$\mathrm{Tr}(\sigma^\mu \bar{\sigma}^\nu) = 2\eta^{\mu\nu}.$$

Here, we list other identities without any provement

$$[k|\gamma^\mu|p\rangle = \langle p|\gamma^\mu|k], \tag{2.8}$$

$$[k|\gamma^\mu|p\rangle^* = [p|\gamma^\mu|k\rangle \qquad \text{(for real moemnta)}. \tag{2.9}$$

and **Fierz identity**

$$\langle 1|\gamma^\mu|2]\langle 3|\gamma_\mu|4] = 2\langle 13\rangle[24] \tag{2.10}$$

will be used in several times. In amplitude calculations, **momentum conservation** is imposed on n particles as $\sum_{i=1}^n p_i^\mu = 0$(here we consider all particles ingoing). Translating by spinor-helicity variable, it becomes

$$\sum_{i=1}^n |i\rangle[i| = 0, \quad \text{i.e.} \quad \sum_{i=1}^n \langle qi\rangle[ik] = 0, \tag{2.11}$$

here q and k are arbitrary light-like vectors.

We end this subsection by introducing one more identity: **Schouten Identity**. It comes from a rather trivial fact: there are no three independent 2-dimensional vectors. So if we have three 2 components angle spinors $|i\rangle$, $|j\rangle$ and $|k\rangle$, we can write one of them as a linear combination of two others

$$|k\rangle = a|i\rangle + b|j\rangle, \qquad \text{for complex a and b.} \tag{2.12}$$

One can contract a $|i\rangle$ and a $|b\rangle$ with the both sides, then a,b can be solved. (2.12) can be cast to the form

$$|i\rangle\langle jk\rangle + |k\rangle\langle ij\rangle + |j\rangle\langle ki\rangle = 0, \tag{2.13}$$

This is Schouten identity and often written with a fourth spinor $\langle r|$

$$\langle ri\rangle[jk] + \langle rk\rangle\langle ij\rangle + \langle rk\rangle\langle ki\rangle = 0. \tag{2.14}$$

We have a similar Schouten identity holding for square spinors

$$[ri][jk] + [rk][ij] + [rj][ki] = 0. \tag{2.15}$$

There is also a important result can be obtained, the **3-particle soecial kinematics**. If we have three light-like vectors satisfying momentum conservation $p_1^\mu + p_2^\mu + p_3^\mu = 0$. Then

$$\langle 12\rangle\langle 21\rangle = 2p_1 \cdot p_2 = (p_1 + p_2)^2 = p_3^2 = 0, \tag{2.16}$$

so either $\langle 12\rangle$ or $[12]$ equals to 0. If we suppose $\langle 12\rangle \neq 0$, then from $\langle 12\rangle[23] = \langle 1|p_2|3] = -\langle 1|p_1 + p_3|3] = 0$, we can conclude that $[23] = 0$. Similarly, we can also obtain $[31] = 0$. Thus, $[12] = [23] = [31] = 0$, which means that the three square spinors are proportional with each other

$$|1] \propto |2] \propto |3] \tag{2.17}$$

or another possibility

$$|1\rangle \propto |2\rangle \propto |3\rangle. \tag{2.18}$$

As a consequence,

1. A non-vanishing on-shell 3-particle amplitude depends only on square brackets or angle brackets.

2. Since for real momenta, angle brackets are complex conjugated with square brackets, so *on-shell 3 point amplitudes are only meanful for complex momenta*(unless it is a constant, like ϕ^3 theory).

2.1.2 Yang-Mills and Color-ordering

Let us consider the Yang-Mills lagrangian

$$\mathcal{L} = -\frac{1}{4} F_{\mu\nu} F^{\mu\nu}, \tag{2.19}$$

with field strength $F_{\mu\nu} = \partial_\mu A_\nu - \partial_\nu A_\mu - \frac{ig}{\sqrt{2}}[A_\mu, A_\nu]$, and $A_\mu = A_\mu^a T^a$. Gauge fields belong to adjoint representation, so the index a runs over $1, 2 \cdots N^2 - 1$ in $SU(N)$ case. The generators are normalized like $\mathrm{Tr}[T^a T^b] = \delta^{ab}$ and $[T^a, T^b] = i\tilde{f}^{abc} T^{c}$[1].

The amplitude-friendly gauge choice is *Gervais-Neveu gauge* with gauge fixing term $\mathcal{L}_{gf} = -\frac{1}{2}\mathrm{Tr}(H_\mu^\mu) = 0$, here $H_{\mu\nu} = \partial_\mu A_n u - \frac{ig}{\sqrt{2}} A_\mu A_\nu$. After gauge fixing, the lagrangian becomes

$$\mathcal{L} = \mathrm{Tr}\left(-\frac{1}{2}\partial_\mu A_\nu \partial^\mu A^\nu - i\sqrt{2} g \partial^\mu A^\nu A_\nu A_\mu + \frac{g^2}{4} A^\mu A^\nu A_\mu A_\nu \right) \tag{2.20}$$

[1]In the usual QFT textbook, $\mathrm{Tr}[T^a T^b] = \frac{1}{2}\delta^{ab}$ and $[T^a, T^b] = i f^{abc} T^c$, with $\tilde{f}^{abc} = \sqrt{2} f^{abc}$ are common choice.

The 3- and 4-gluon vertices involve $\tilde{f}^{abc}$ and $\tilde{f}^{abi}\tilde{f}^{icd}$+permutations, respectively, each dressed up with kinematic factors. The amplitudes constructed from these rules can be organized into different group theory structures. For example, the color factors of the s-, t-, and u-channel diagram of the 4-gluon tree amplitude are

$$c_s = \tilde{f}^{a_1 a_2 b}\tilde{f}^{b a_3 a_4}, \quad c_t = \tilde{f}^{a_4 a_1 b}\tilde{f}^{b a_2 a_3}, \quad c_u = \tilde{f}^{a_1 a_3 b}\tilde{f}^{b a_2 a_4} \tag{2.21}$$

and the four point interaction just gives a sum of contributions from c_s, c_t and c_u. And because of the Jacobi identity, we have

$$c_s = c_t + c_u. \tag{2.22}$$

And the color factor can be written by the trace of product of generators

$$i\tilde{f}^{abc} = \mathrm{Tr}([T^a, T^b]T^c), \tag{2.23}$$

where T^a are generators of fundamental representation. Moreover, in $SU(N)$, we have a Fierz identity

$$\sum_a T^a_{ij} T^a_{kl} = \delta_{il}\delta_{kj} - \frac{1}{N}\delta_{ij}\delta_{kl}. \tag{2.24}$$

This identity is easier understood as matrix form like

$$\mathrm{Tr}\{T^a A\}\mathrm{Tr}\{T^a B\} = \mathrm{Tr}\{AB\} - \frac{1}{N}\mathrm{Tr}\{A\}\mathrm{Tr}\{B\}, \tag{2.25}$$

and

$$\mathrm{Tr}\{AT^a BT^a\} = \mathrm{Tr}\{A\}\mathrm{Tr}\{B\} - \frac{1}{N}\mathrm{Tr}\{AB\}. \tag{2.26}$$

Then it can be used to simplify the calculation.

For example, the 4 gluon s-channel gives us

$$\tilde{f}^{a_1 a_2 b}\tilde{f}^{b a_3 a_4} = \mathrm{Tr}(T^{a_1}T^{a_2}T^{a_3}T^{a_4}) - \mathrm{Tr}(T^{a_2}T^{a_1}T^{a_3}T^{a_4}) - \mathrm{Tr}(T^{a_1}T^{a_2}T^{a_4}T^{a_3}) + \mathrm{Tr}(T^{a_2}T^{a_1}T^{a_4}T^{a_3}). \tag{2.27}$$

Similarly, three other diagrams can also be written in terms of single trace. Therefore, the full 4-point amplitude can be rewritten like

$$\mathcal{A}_{4,\mathrm{tree}} = g^2(A_4[1234]\mathrm{Tr}(T^{a_1}T^{a_2}T^{a_3}T^{a_4}) + \text{perms of } (234)) \tag{2.28}$$

here the subamplitudes $A_4[1234], A_4[1243]$, etc. are called **color-ordereed ampltitudes**. This concept can be easily generalized to tree-level n-point case

$$\mathcal{A}_{n,\mathrm{tree}} = g^{n-2}\sum_\sigma A_n[1, \sigma(2, 3\cdots n)]\mathrm{Tr}(T^{a_1}T^{\sigma(a_2\cdots}T^{a_n)}) \tag{2.29}$$

where the sun is taken over the $(n-1)!$ trace basis (considering the cyclic property of trace).

Actually, the number of independent basis can be reduced to $(n-3)!$, called Del Duca-Dixon-Maltoni (DDM) color decomposition [2]. But it has no tight relation with this paper, so here we do not offer more detailed explanation for it.

The color-ordered amplitude $A_n[1,2...n]$ is calculated in terms of diagrams with no lines crossing(planar diagrams) and the ordering of the external lines fixed as given 1, 2, 3,..., n. Here, we directly give the final result for 3-point color-ordered amplitudes without any intermediate calculating process. And in this full paper, we mainly consider the helicity amplitudes which will be explained later, so we need to clarify the helicity configuration.

For 3-point, there are only two non-vanishing configurations

$$A_3[1^-,2^-,3^+] = \frac{\langle 12\rangle^3}{\langle 23\rangle\langle 31\rangle} \tag{2.30}$$

and

$$A_3[1^+,2^+,3^-] = \frac{[12]^3}{[23][31]}. \tag{2.31}$$

It has been known that there is a compact formula for n-point gluon color-ordered amplitudes — ***Parke - Talyor Formula***

$$A_n[1^+\cdots i^-\cdots j^-\cdots n^+] = \frac{\langle ij\rangle^4}{\langle 12\rangle\langle 23\rangle\cdots\langle n1\rangle}. \tag{2.32}$$

We will prove this formula in the next subsection.

The color-ordered amplitudes have a number of properties

1. *Cyclic*: It follows from the cyclic property for trace that $A_n[12\cdots n] = A_n[2n\cdots 1]$
2. *Reflection*: $A_n[12\cdots n] = (-1)^n A_[n\cdots 21]$
3. The $U(1)$ *decoupling identity*:

$$A_n[123\cdots n] + A_n[213\cdots n] + A_n[231\cdots n] + \cdots + A_n[23\cdots 1n] = 0 \tag{2.33}$$

The trace basis (2.29) is overcomplete implies that there are further linear relations among these subamplitudes, which are called ***Kleiss - Kuiff(KK) relations***

$$A_n[1,\{\alpha\},n,\{\beta\}] = (-1)^{|\beta|}\sum_{\sigma\in \mathrm{OP}(\{\alpha\},\{\beta^T\})} A_n[1,\sigma,n] \tag{2.34}$$

where β^T denotes the reverse ordering of the labels $\{\beta\}$ and the sum is over ordered permutations "OP", means permutations of the labels in the joined set $\{\alpha\}\cup\{\beta^T\}$ in which the ordering within $\{\alpha\}$ and $\{\beta\}^T$ is preserved.

Consider a 5-point case as an example. Taking the LHS to be $A_5[1,\{2\},5,\{3,4\}]$, we have $\{\alpha\}\cup\{\beta^T\} = \{2\}\cup\{4,3\}$, so the ordered permutations σ refers to $\{243\},\{423\},\{432\}$. Thus

the KK relation reads

$$A_5[12534] = A_5[12435] + A_5[14235] + A_5[114325]. \tag{2.35}$$

The KK relations combine with cyclic, reflection, and $U(1)$ decoupling identities reduce the number of independent basis to $(n-2)!$. However, there are further linear relations called ***BCJ relations*** – named after Bern, Carrasco and Johansson, which further reduce the number to $(n-3)!$.

Although I will not show the derivation of BCJ relations, I would like to give some examples

$$s_{14}A_4[1234] - s_{13}A_4[1243] = 0, \tag{2.36}$$

$$s_{12}A_5[21345]s_{23}A_5[13245] - (s_{23}+s_{24})A_5[13425] = 0. \tag{2.37}$$

2.2 Little group scalling

The rich structure of scattering amplitudes can be originated from a fundamental question — "What is a particle?" — which relates directly to Wigner's Little group notation, characterizing how particles transform under Lorentz symmetry. Following this thought, we think particle as a unitary representation of Poincaré group, which is the symmetry group of our spacetime. We use two labels to denote a one-particle state, one is the momentum p^μ, another is σ representing other labels the particle ca carry.

We start from a one-particle state $|k;\sigma\rangle$ with reference momentum k. Another momentum p is related by the lorentz transformation $L(p;k)$, $p = L(p;k)k$. Obviously, this Lorentz transformation is not unique because there exist Lorentz transformations keeping p invariant, called "Little group transformation". We assume that there exist a unitary representation for the Lorentz group, the operator in Hillbert space are denoted like $U(\Lambda)$.

Then we simply *define* the one-particle state with momentum p as

$$|p;\sigma\rangle = U(L(p;k))|k;\sigma\rangle. \tag{2.38}$$

Having made this definition, we can compute how the state transformed under a general Lorentz transformation

$$U(\Lambda)|p,\sigma\rangle = U(\Lambda)U(L(p;k))|k,\sigma\rangle = U(L(\Lambda p;k))U(L^{-1}(\Lambda p;k)\Lambda L(p;k))|k,\sigma\rangle\,. \tag{2.39}$$

here we use the fact $U(\Lambda_1\Lambda_2) = U(\Lambda_1)U(\Lambda_2)$. Notice that $W(\Lambda,p,k)$ is not a general transformation but keep the momentum k invariant $Wk = k$. This subgroup of Lorentz group is called little group. Thus we must have

$$U(W(\Lambda,p,k))|k;\sigma\rangle = D_{\sigma\sigma'}(W(\Lambda,p,k))|k,\sigma'\rangle, \tag{2.40}$$

where $D_{\sigma\sigma'}$ is the representation for little group. Then, p should transformed like

$$U(\Lambda)|p,\sigma\rangle = D_{\sigma\sigma'}(W(\Lambda,p,k))|\Lambda p,\sigma'\rangle \tag{2.41}$$

The scattering amplitudes for n particle should keep invariant under Poincaré transformation – translation invariance and Lorentz invariance

$$\mathcal{M}(p_a,\sigma_a) = \delta^D(p_1^\mu + \cdots + p_n^\mu)\mathcal{M}(p_a,\sigma_a) \tag{2.42}$$

$$\mathcal{M}^\Lambda(p_a,\sigma_a) = \prod_a (D_{\sigma\sigma'})\mathcal{M}((\Lambda p)_a,\sigma_a') \tag{2.43}$$

In D spacetime dimensions, the little group for massive particles is $SO(D-1)$. For massless particles the little group is the the group of Euclidean symmetries in (D - 2) dimensions, which is $SO(D-2)$.In this article, we mainly discuss massless particles scattering in 4 dimension spacetime, so the little group is $SO(2) \backsimeq U(1)$.

Then from the definition of spinor-helicity variable(2.1), we can notice that there is an ambiguity here. The momentum is invariant under the following redefinition

$$\lambda \to t^{-1}\lambda, \qquad \tilde{\lambda} \to t\tilde{\lambda}, \qquad t \in \mathbb{C} \tag{2.44}$$

same for

$$|\lambda\rangle \to t^{-1}|\lambda\rangle, \qquad |\lambda] \to t|\lambda] \tag{2.45}$$

. This scale perfectly matches the $U(1)$ little group transformation, so we can identify this rescale as the little group transformation. The scattering amplitudes should transform covariantly under little group scaling like (2.43), so

$$\mathcal{A}_n(\{|1\rangle,|1],h_1\},\ldots\{t_i^{-1}|i\rangle,t_i|i],h_i\},\ldots) = t_i^{2h_i}\mathcal{A}_n \tag{2.46}$$

where h_i refers to the helicity of particles. As an example, consider the QED amplitude, $A_3(f^-\bar{f}^+\gamma^-) = e\frac{\langle 13\rangle^2}{\langle 12\rangle}$. For the negative helicity photon (particle 3), we obtain $t_3^{-2} = t_3^{2(-1)}$. We will see that little group scaling plays a significant role in 3-particle amplitudes.

3-particle amplitudes

By 3-particle special kinematics, we have known that on-shell 3-point amplitudes depends on either square brackets or angle brackets. We suppose that it only depends on angle brackets. We can write down the general ansatz

$$A_3(1^{h_1},2^{h_2},3^{h_3}) = c\langle 12\rangle^{x_{12}}\langle 13\rangle^{x_{13}}\langle 23\rangle^{x_{23}}, \tag{2.47}$$

where c is just a constant. Little group scaling (2.46) tell us that

$$t_1^{2h_1}A_3(1^{h_1},2^{h_2},3^{h_3}) = ct_1^{-x_{12}}t_1^{-x_{13}}\langle 12\rangle^{x_{12}}\langle 13\rangle^{x_{13}}\langle 23\rangle^{x_{23}}. \tag{2.48}$$

We can obtain

$$2h_1 = -x_{12} - x_{13} \tag{2.49}$$

Similarly, we can also obtain

$$2h_2 = -x_{12} - x_{23}, \qquad 2h_3 = -x_{13} - x_{23}. \tag{2.50}$$

Then all index can be solved from this system of equations, so that

$$A_3^{h_1h_2h_3} = c\langle 12\rangle^{h_3-h_1-h_2}\langle 31\rangle^{h_2-h_1-h_3}\langle 23\rangle^{h_1-h_2-h_3} \qquad h_1+h_2+h_3<0 \tag{2.51}$$

$$A_3^{h_1h_2h_3} = c'[12]^{h_1+h_2-h_3}[23]^{h_2+h_3-h_1}[31]^{h_3+h_1-h_2} \qquad h_1+h_2+h_3>0 \tag{2.52}$$

This means that ***all massless 3-point amplitudes are completely fixed by little group scaling!***

We have shown the 3-point QED amplitudes. So now we can consider something different – 3-point gluon amplitudes with 2 same helicities and 1 different helicity. Then we can determine the amplitudes from (2.51) (2.52)

$$A_3(g_1^-, g_2^-, g_3^+) = g\frac{\langle 12\rangle^3}{\langle 23\rangle\langle 31\rangle}, \quad A_3(g_1^+, g_2^+, g_3^-) = g\frac{[12]^3}{[23][31]} \tag{2.53}$$

Here it need some efforts to explain about the condition after equation (2.51) and (2.52).If we assume the amplitude $A_3(g_1^-, g_2^-, g_3^+)$ depending on square brackets, so can obtain a different expression

$$A_3(g_1^-, g_2^-, g_3^+) = g^{'}\frac{[31][23]}{[12]^3}, \tag{2.54}$$

to distinguish these two possibilities, we need to use **dimension analysis**. From (2.7), we can know that both square brackets and angle brackets have mass-dimension 1. Thus the kinematic factor of amplitude (2.53) has mass-dimension 1, compatible with the interaction term $AA\partial A$ in $\mathrm{Tr}F_{\mu\nu}F^{\mu\nu}$. But the mass-dimension of kinematic factor in (2.54) is (-1), so it should come from the interaction term like $g^{'}AA\frac{1}{\Box}A$. Here, we only consider the local field theory, so this kind of interaction should be discarded.

The combination of ***little group scaling*** and ***locality*** uniquely fixes the massless 3-point amplitudes. In general,

$$\text{An n-point amplitude in D=4 spacetime have mass-dimension 4 - n.} \tag{2.55}$$

Although we discard the amplitude (2.54), the coupling s¥constant $g^{'}$ have mass-dimension 2, so (2.54) has the correct mass-dimension as (2.53).

How about the gluon amplitude with all minus helicities? The formula (2.51) immediately

tells that it should equal to

$$A_3(g_1^-, g_2^-, g_3^-) = g'' \langle 12\rangle\langle 23\rangle\langle 31\rangle. \tag{2.56}$$

The kinematic part has mass-dimension 3 and reveals that:

1. The coupling constant g'' must have mass-dimension -2.

2. This must come from an interaction term with 3 derivatives like $(\partial A)^3$.

Furthermore, kinematic part has the antisymmetry under the exchange of gluon momenta, so the coupling constant should also have this antisymmetry in order to satisfy the Bose statics as is of course the pure Yang-Mills case. The natural candidate of this amplitude is a dimension 6 operator $\mathrm{Tr}F^\mu_\nu F^\nu_\lambda F^\lambda_\mu$.

2.3 MHV Classification

It has been well known that the all-plus tree-level gluon amplitudes vanish

$$\text{tree-level gluon amplitues}: \quad A_n[1^+, 2^+, \cdots, n^+] = 0 \quad \text{and} \quad A_n[1^+, 2^+, \cdots, n^-] = 0 \tag{2.57}$$

This conclusion holds for the case with all helicities flipped:

$$\text{tree-level gluon amplitues}: \quad A_n[1^-, 2^-, \cdots, n^-] = 0 \quad \text{and} \quad A_n[1^-, 2^-, \cdots, n^+] = 0 \tag{2.58}$$

In supersymmetric Yang-Mills theories, these results hold for all loop order, so actually it is a special case for SYM.

If we flip one more helicit, the situation becomes quite different. Amplitudes $A_n[1^-, 2^-, 3^+, \cdots, n^+]$ does not equal to 0 and is quite important called **MHV amplitudes**. The gluon amplitudes with two negative helicities and n - 2 positive helicities are called ***maximally helicity violating*** – or simply ***MHV*** for short. The concept "maximally helicity violating" comes from thinking a $2 \to n-2$ scattering process. Because of crossing symmetry, the outgoing particle with positive(negtive) helicity is equivalent with an ingoing particle with negative(positive) helicty. So if we consider the process $A_n[1^+, 2^+, \cdots, n^+]$ with all particle ingoing. It crosses over to $1^+2^-+ \to 3^- \cdots n^-$ with two ingoing particles and n-2 outgoing particles, that's the reason we call it "helicity violating". We have known that the process in which the most we can violate helicity is $1^+2^+ \to 3^+4^+5^- \cdots n^-$, which is equivalent to amplitudes $A_n[1^+2^+3^-4^-5^+ \cdots n^+]$, therefore it is the *maximally helicity violating* process.

As we have shown in the last subsection, the MHV gluon tree amplitudes are given by Parke - Talyor formula

$$A_n[1^+ \cdots i^- \cdots j^- \cdots n^+] = \frac{\langle ij\rangle^4}{\langle 12\rangle\langle 23\rangle \cdots \langle n1\rangle} \tag{2.59}$$

The MHV amplitudes are the important blocks for scattering amplitudes in (super)Yang-Mills theory. They are simplest amplitudes, and the next-to simplest are called **Next-to-MHV** amplitudes, or just **NMHV**. This refers to scattering process for which two 2 positive gluons scatter into 3 positive gluons and n-5 negative gluons. Similarly, we can define N^k**MHV** amplitudes. For anti-MHV amplitudes with all helicities flipping, we have a formula

$$A_n[1^- \cdots i^+ \cdots j^+ \cdots n^-] = \frac{[ij]^4}{[12][23]\cdots[n1]}. \tag{2.60}$$

2.4 BCFW recursion relation

The BCFW recursion relation was introduced in 2005 by Britto, Cachazo, and Feng, and later extended with Witten. It provided a novel way to compute tree-level scattering amplitudes by analytically continuing external momenta into the complex plane and expressing higher-point amplitudes recursively in terms of lower-point ones. This on-shell approach uncovered surprising simplicity in gauge theory amplitudes and offered an alternative to the traditional Feynman diagram expansion. The method was inspired in part by Witten's twistor string theory and the MHV diagram program. In parallel, off-shell recursion relations were also being explored, especially in background field methods and Berends-Giele recursion, which organize amplitudes based on off-shell currents. While off-shell methods remain useful in certain computational frameworks, the BCFW recursion highlighted the power of staying strictly on-shell, leading to a deeper understanding of symmetry, analyticity, and the geometry of scattering processes. It has since become a cornerstone of modern amplitude research.

Beyond BCFW, other on-shell recursion relations have also emerged—for instance, the KLT relations linking gauge and gravity amplitudes, and the double copy structure as well as recursion for theories with special helicity configurations or massive particles. Together, these developments form the foundation of modern amplitude methods, emphasizing physical principles like unitarity, analyticity, and factorization over traditional Lagrangian-based techniques.

2.4.1 Complex shift and Relation from Simple Cauchy's Theorem

An on-shell amplitude(each external leg satisfies on-shell condition) is labeled by their external momentum p_μ and hilicity h_i. Here we only consider the massless particles $p_i^2 = 0$, for $i = 1, 2, \cdots, n$. And momentum conservation $\sum_{i=1}^n p_i^\mu = 0$ should hold.

First, let us consider the most general case. We need to introduce n complex-valued vectors r_i^μ subject to

- $\sum_{i=1}^n r_i^\mu = 0$,
- $r_i \cdot r_j = 0$ for all $i, j = 1, 2, \cdots, n$. In particular, $r_i^2 = 0$,
- $p_i \cdot r_i = 0$ for each i(no sum).

These vectors r_i are used to define n shifted momentum

$$\hat{p}_i^\mu \equiv p_i^\mu + z r_i^\mu \quad \text{with} \quad z \in \mathcal{C} \tag{2.61}$$

Note that, by imposing these constraints,

- Momentum conservation holds for the shifted momentum: $\sum_{i=1}^n \hat{p}_i^\mu = 0$,
- We have $\hat{p}_i^2 = 0$, so each shifted momentum still keep on-shell
- For a non-trival [2] subset of momentum $\{p_i\}_{i\in I}$, define $P_i^\mu = \sum_{i\in I} p_i^\mu$. Then $\hat{P}_I^2$ is **linear** in z:

$$\hat{P}_I^2 = P_I^2 - 2zP_I \cdot k = -\frac{P_I^2}{z_I}(z - z_I) \tag{2.62}$$

  beacuse the z^2 term vanishes. We can write

$$\hat{P}_I^2 = -\frac{P_I^2}{z_I}(z - z_I) \qquad with z_I = \frac{P_I^2}{2P_I \cdot k} \tag{2.63}$$

If we consider the original amplitude A_n in terms of the shifted momentum $\hat{p}_i^\mu$ instead of original momentum. Then the amplitude can be seen as a holomorphic function of z. Actually, if we set $z = 0$, we can obtain the origin ampltide $A_n = \hat{A}_n(z = 0)$.

In this paper, we only focus on the tree-level scatterung amplitudes, in which case the analytic structure becomes quite simple. The tree amplitudes does not have any branch cuts – there are no logs, no square roots, etc.. The tree-level amplitude is a rational function of Lorentz invariant kinematic quantities, like the contraction between momentum or momentum and polarization vector. Therefore, the analytic structure can be completely captured by its single poles in the complex z plane. To see that all of the poles are single, we just need to notice that we can only ontain poles from propagators. But we have seen that all of the poles can be dertermined by (2.63). So $1/\hat{P}_I^2$ gives a single pole at z_I, and for generic momentum, $P_I^2 \neq 0$(propagator is off-shell) so $z_I \neq 0$. Hence, $\hat{A}_n(z)$ only has single poles away from the orignal poine $z = 0$.[3]

Then let us turn to define a new holomorphic function $\frac{\hat{A}_n(z)}{z}$ in the complex plane. We can pick a contour surrounding the original point $z = 0$ which is a single pole of this function. The residue of this single pole can be easily computed

$$\text{Res}|_{z=0} \frac{\hat{A}_n(z)}{z} = \hat{A}_n(z = 0) = A_n, \tag{2.64}$$

It is just the unshifted amplitude what we want to compute at the begining.

[2] non-trival here means at least two and no more than n-2 such that $P_I^2 \neq 0$

[3] Here we need to impose locality to ensure all of the poles can be determined by the propagators.

Also, we can choose another countour surrounding all single poles, then Cauchy's theorem just tell us

$$A_n = -\sum_{z_I} \text{Res}_{z=z_I} \frac{\hat{A}_n(z)}{z} + B_n \,, \tag{2.65}$$

where the B_n is the residue at $z = \infty$ infinity, called bounday term. By taking $z \to 1/\omega$, it is easy to notice that B_n is the $O(z^0)$ term in the $z \to \infty$ expansion of A_n.

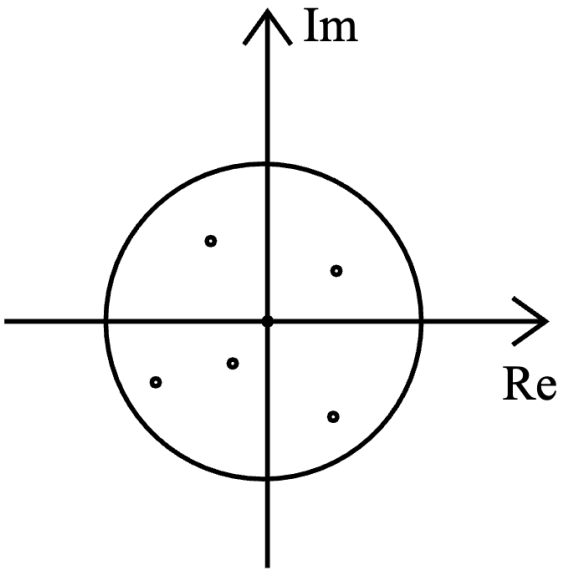

Figure 1: Cauchy Theorem

Now, at the position of z_I pole, the propagator $1/\hat{P}_I^2$ gose on-shell. The unitarity has a tight relation with I poles in the S-matrix with on-shell intermediate states.

$$G_n(p_1, \ldots, p_n) = (2\pi)^4 \, \delta^4 \left(\sum p \right) \frac{i}{p_\Psi^2 - m_\Psi^2 + i\varepsilon} \mathcal{M}_\Psi^{1,r} \, \mathcal{M}_\Psi^{r+1,n\dagger} + \text{extra} \tag{2.66}$$

where "extra" refers to anything else that contributes. This equation says that Green's functions always have poles when on-shell intermediate particles can be produced.

Then, in the on-shell limit, the shifted amplitude *factorizes* into two on-shell parts

$$\hat{A}_n(z) \quad \xrightarrow{z \text{ near } z_I} \quad \hat{A}_L(z_I) \frac{1}{\hat{P}_I^2} \hat{A}_R(z_I) = -\frac{z_I}{z - z_I} \hat{A}_L(z_I) \frac{1}{P_I^2} \hat{A}_R(z_I) \tag{2.67}$$

This makes it easy to compute the residue at $z = z_I$

$$-\text{Res}|_{z=z_I} \frac{\hat{A}_n(z)}{z} = -(z - z_I) \frac{z_I}{z(z - z_I)}|_{z=z_I} \hat{A}_L(z_I) \frac{1}{P_I^2} \hat{A}_R(z_I) = \hat{A}_L(z_I) \frac{1}{P_I^2} \hat{A}_R(z_I) \tag{2.68}$$

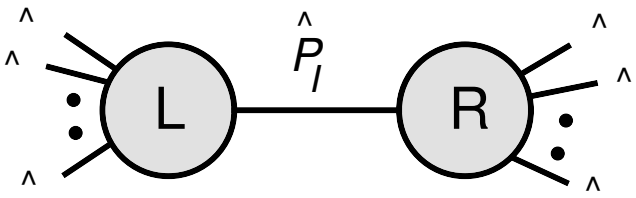

Figure 2: factorization

Note that, as opposed to Feynman diagrams for which the intermediate propagator does not equal to 0, here the intertal line $\hat{P}_I^2$ of Figure 2 does equal to 0. And the blobs which refer to subamplitudes are ***on-shell amplitudes***. In the diagrammatic representation Figure 2, the internal line is assigned the usual scalar propagator $1/P_I^2$, evaluated using unshifted momenta. Since each subamplitude involves fewer than n external particles, all the residues at finite z can be expressed entirely in terms of lower-point on-shell amplitudes. This fundamental idea underlies the construction of the recursion relations.

The contribution B_n does affect a lot, and it has no similar general expression in trems of lower-point amplitudes. Although in some cases, the boundary term B_n can be computed, but there is not a general method to compute it. Thus, in most applications, we always assumes, or better, prove that $B_n = 0$. This is often modified by demonstrating stronger statement that

$$\hat{A}_n(z) \to 0 \quad \text{for} \quad z \to \infty. \tag{2.69}$$

If (2.69) holds, we state the shift is ***valid***.

For a valid shift, the n-point amplitudes can be recursively computed interms of lower-point amplitude

$$A_n = \sum_{\text{diagrams } I} \hat{A}_{\text{L}}(z_I) \frac{1}{P_I^2} \hat{A}_{\text{R}}(z_I) = \sum_{\text{diagrams } I}$$ 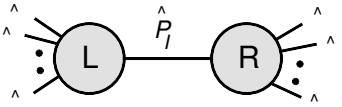 .

(2.70)

where I means all possible factorization channels. We did not use any $D = 4$ spacetime property, so this recursion relation can be utilized to general D dimension spacetime.

2.4.2 BCFW recursion relation

In the last section, we introduce the recursion relation with all momentum shifted. But actually, some of the shift vectors r_i^μ can be choose to 0. The BCFW shift is a kind of special shift for which only two momentum are shifted, called i and j. In D=4 spacetime diension, the shift is implemented

$$\hat{p}_i(z) = p_i - zq, \qquad \hat{p}_j(z) = p_j + zq \tag{2.71}$$

so momentum conservation is kept and the hold for on-shell condition require ot impose

$$q^2 = q \cdot p_i = q \cdot p_j = 0\,. \tag{2.72}$$

This shift can be implemented in terms of spinor-helicity variable as

$$|\hat{i}] = |i] - z\,|j]\,, \qquad |\hat{j}] = |j]\,, \qquad |\hat{i}\rangle = |i\rangle\,, \qquad |\hat{j}\rangle = |j\rangle + z|i\rangle\,. \tag{2.73}$$

No other spinors are shifted, this kind of shift are called $[i,j\rangle$ shift(it is worth to mention that $[i,j\rangle$ shift is completely different with $[j,i\rangle$ shift).Note that $[\hat{i}k]$ and $\langle\hat{j}k\rangle$ are linear in z for $k \neq i,j$, while $\langle\hat{i}\hat{j}\rangle = \langle ij\rangle$, $[\hat{i}\,\hat{j}] = [ij]$, $\langle\hat{i}k\rangle = \langle ik\rangle$, and $[\hat{j}k] = [jk]$ remain unshifted. In the literature, the BCFW deformation is usually written in the above spinor form. However, the momentum form (2.71) provides another perspective.

The BCFW recursion relation takes the form

$$A_n \;=\; \sum_{\text{diagrams }I} \hat{A}_{\rm L}(z_I)\,\frac{1}{P_I^2}\,\hat{A}_{\rm R}(z_I) \;=\; \sum_{\text{diagrams }I}$$

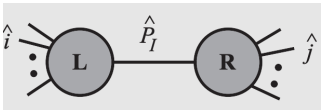

. (2.74)

Beforing going into the apllication of BCFW, let us first consider the large-z behavior. In pure Yang-Mills case, it has been proved that the color-ordered gluon tree-level amplitudes behave like the following manner [3]

$[i,j\rangle$	$[-,-\rangle$	$[-,+\rangle$	$[+,+\rangle$	$[+,-\rangle$
$\hat{A}_n(z) \sim$	$\frac{1}{z}$	$\frac{1}{z}$	$\frac{1}{z}$	z^3

If i,j are not adjacent, one obtains an extra $1/z$ in each case. Thus any one of shifts , $[-,-\rangle, [-,+\rangle, [+,+\rangle$ are valid but $[+,-\rangle$ is not valid. This is a quite non-trival result. If we consider more general case [4]

$$p_i(z) = p_i + z\lambda_i\tilde{\lambda}_j, \quad p_j(z) = p_j - z\lambda_i\tilde{\lambda}_j, \Rightarrow \begin{cases} A(z) \to z^{-2}, & i,j \text{ not nearby} \\ A(z) \to z^{-1}, & i,j \text{ nearby} \end{cases}$$

$$p_i(z) = p_i + z\lambda_i\tilde{\lambda}_k \ (k \neq j), \quad p_k(z) = p_k - z\lambda_i\tilde{\lambda}_k, \Rightarrow \begin{cases} A(z) \to z^{-2}, & i,k \text{ not nearby} \\ A(z) \to z^{-1}, & i,k \text{ nearby} \end{cases}$$

$$p_i(z) = p_i + z\lambda_k\tilde{\lambda}_i \ (k \neq j), \quad p_k(z) = p_k - z\lambda_k\tilde{\lambda}_i, \Rightarrow \begin{cases} A(z) \to z^2, & i,k \text{ not nearby} \\ A(z) \to z^3, & i,k \text{ nearby} \end{cases}$$

$$p_k(z) = p_k + z\lambda_l\tilde{\lambda}_k, \quad p_l(z) = p_l - z\lambda_l\tilde{\lambda}_k, \quad k,l \neq i,j \Rightarrow \begin{cases} A(z) \to z^{-2}, & l,k \text{ not nearby} \\ A(z) \to z^{-1}, & l,k \text{ nearby} \end{cases} \tag{2.75}$$

where i, j are negetive helicities. Then we can go forward to the provement of Parke - Talyor formula by using BCFW recursion relation. First, we can notice that the formula

$$A_n[1^+ \cdots i^- \cdots j^- \cdots n^+] = \frac{\langle ij\rangle^4}{\langle 12\rangle\langle 23\rangle \cdots \langle n1\rangle} \tag{2.76}$$

holds for $n = 3$ case, and we start the provement by induction from 3-point. For specific n, we suppose (2.76) holds for amplitudes with external legs less than n. Then we can writte down the n-point amplitude $A_n[1^-2^-3^+ \cdots n^-]$ with BCFW shift $[1, 2\rangle$

$$\begin{aligned} A_n[1^-2^-3^+ \ldots n^+] &= \sum_{k=4}^{n} \quad \text{ 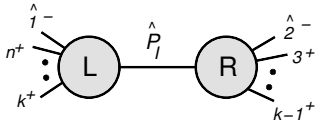 } \\ &= \sum_{k=4}^{n} \sum_{h_I=\pm} \hat{A}_{n-k+3}\Big[\hat{1}^-, \hat{P}_I^{h_I}, k^+ \ldots, n^+\Big] \frac{1}{P_I^2} \\ &\quad \times \hat{A}_{k-1}\Big[-\hat{P}_I^{-h_I}, \hat{2}^-, 3^+ \ldots, (k-1)^+\Big]. \end{aligned} \tag{2.77}$$

The internal momentum can be evaluated as $P_I = p_2 + p_3 + \cdots + p_{k-1}$ and $\hat{P}_I = \hat{p}_2 + p_3 + \cdots + p_{k-1}$ if we choos $k = 4, 5, \cdots, n$. Notice that there are no such diagrams in which the $\hat{p_1}$ and $\hat{p}_2$ locate at the same side, whereby there are no z independence, so that we can not obtain any single pole in the complex plane. And because we are computing the color-ordered amplitudes, only diagrams that preserve the color-ordering of the external states are included. Note that we explicitly include the sum over all possible helicity assignments for the particle exchanged on the on-shell internal line. Specifically, if the exchanged gluon appears as an outgoing particle with negative helicity in the left subamplitude, it will correspondingly appear as an outgoing gluon with positive helicity in the right subamplitude.

We have known that the color-amplitudes $A_n[- + +c \cdots +]$ equals to 0, except for $n = 3$

case. So (2.77) can be computed like

$$A_n[1^-2^-3^+\dots n^+] = \quad + \quad$$

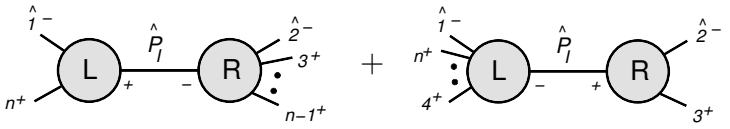

$$= \hat{A}_3\Big[\hat{1}^-, -\hat{P}^+_{1n}, n^+\Big]\,\frac{1}{P^2_{1n}}\,\hat{A}_{n-1}\Big[\hat{P}^-_{1n}, \hat{2}^-, 3^+\dots(n-1)^+\Big]$$
$$+\ \hat{A}_{n-1}\Big[\hat{1}^-, \hat{P}^-_{23}, 4^+\dots, n^+\Big]\,\frac{1}{P^2_{23}}\,\hat{A}_3\Big[-\hat{P}^+_{23}, \hat{2}^-, 3^+\Big]\,. \tag{2.78}$$

Notice that in the first diagram of (2.78), there is a 3-point subamplitude

$$\hat{A}_3\Big[\hat{1}^-, -\hat{P}^+_{1n}\,, n^+\Big] \;=\; \frac{[\hat{P}_{1n}\,n]^3}{[n\hat{1}][\hat{1}\hat{P}_{1n}]}\,. \tag{2.79}$$

here we take the convention of analytic continuation like

$$|-p\rangle = -|p\rangle, \qquad |-p] = +|p]. \tag{2.80}$$

Because the propagator satisfies the on-shell condition, so we can obtain

$$\hat{P}^2_{1n} = 0 = 2\hat{p}_1\cdot p_n = \langle\hat{1}n\rangle[n\hat{1}], \tag{2.81}$$

because we take the $[1,2\rangle$ shift, so that $|\hat{1}\rangle = |1\rangle$. And the angle bracket $\langle 1n\rangle$ can not equal to 0, so that

$$[\hat{1}n] = 0 \qquad \Longrightarrow \qquad z = \frac{[1n]}{[2n]}, \tag{2.82}$$

so the potion of pole is determined by the on-shell propagator. Also, we can compute like

$$|\hat{P}_{1n}\rangle[\hat{P}_{1n}\,n] = -\hat{P}_{1n}|n] \;=\; -(\hat{p}_1 + p_n)|n] \;=\; |1\rangle[\hat{1}n] \;=\; 0\,, \tag{2.83}$$

we can conclude $[\hat{P}_{1n}\,n] = 0$ because of $[\hat{1}n] = 0$ and $|\hat{P}_{1n}\rangle \neq 0$. So the 3-point amplitude (2.79) has both a vanishing numerator and denominator, with the numerator vanishing one order faster. We conclude that special 3-point kinematics force $\hat{A}_3\Big[\hat{1}^-, -\hat{P}^+_{1n}\,, n^+\Big]$. So the contribution from the first diagram in (2.78)vanishes.

For the second diagram in (2.78), we will not obtain the vanishing result, because it is an anti-MHV amplitude with angle spinor $|2\rangle$ shifted. Henceforth, the seemingly complicated summation (2.78) redeuce to a single diagram. This is one merit of BCFW recursion relation.

Then the amplitude can be evaluated like

$$A_n[1^-2^-3^+\dots n^+] = \quad = \hat{A}_{n-1}\Big[\hat{1}^-, \hat{P}_{23}^-, 4^+, \dots, n^+\Big]\,\frac{1}{P_{23}^2}\,\hat{A}_3\Big[-\hat{P}_{23}^+, \hat{2}^-, 3^+\Big]\,. \tag{2.84}$$

By using the lower point Parke - Talyor formula which assune to hold, the amplitude can be written like

$$A_n[1^-2^-3^+\dots n^+] \;=\; \frac{\langle\hat{1}\hat{P}_{23}\rangle^4}{\langle\hat{1}\hat{P}_{23}\rangle\langle\hat{P}_{23}\,4\rangle\langle 45\rangle\cdots\langle n\hat{1}\rangle} \times \frac{1}{\langle 23\rangle[23]} \times \frac{[3\hat{P}_{23}]^3}{[\hat{P}_{23}\,\hat{2}][\hat{2}3]}\,. \tag{2.85}$$

This formula can be further simplified by using

$$\langle\hat{1}\hat{P}_{23}\rangle[3\hat{P}_{23}] = -\langle\hat{1}\hat{P}_{23}\rangle[\hat{P}_{23}3] = -\langle 1|\hat{p}_2 + p_3|3] = -\langle 1|\hat{p}_2|3] = \langle 12\rangle[32] \tag{2.86}$$

here we use the fact $|\hat{1}\rangle = |1\rangle$ and $\langle 1\hat{2}\rangle = \langle 12\rangle$. And similarly , for the demoninator we have the similar result

$$\langle\hat{P}_{23}4\rangle[\hat{P}_{23}\hat{2}] = -\langle 4\hat{P}_{23}\rangle[\hat{P}_{23}\hat{2}] = -\langle 4|\hat{p}_2 + p_3|2] = \langle 34\rangle[32] \tag{2.87}$$

here we use the fact $|\hat{2}] = |2]$.

Then the full amplitude equals to

$$A_n[1^-2^-3^+\dots n^+] = \frac{\langle 12\rangle^3[32]^3}{\langle 34\rangle[32]\langle 23\rangle[23][23]\langle 45\rangle\cdots\langle n1\rangle} \tag{2.88}$$

$$= \frac{\langle ij\rangle^4}{\langle 12\rangle\langle 23\rangle\cdots\langle n1\rangle} \tag{2.89}$$

so we finish the provement of Parke - Talyor formula by utlizing BCFW recursion relation.

Notice that this formula only holds for MNH anplitudes. For NMHV amplitudes, of coure we can still use BCFW recusion relation to similarly compute them. Here, I only show the result of 6-gluon NMHV tree amplitude.

$$A_6[1^-2^-3^-4^+5^+6^+] \;=\; \quad + \quad \tag{2.90}$$

diagram A diagram B

$$= \frac{\langle 3|1+2|6]^3}{P_{126}^2[21][16]\langle 34\rangle\langle 45\rangle\langle 5|1+6|2]} + \frac{\langle 1|5+6|4]^3}{P_{156}^2[23][34]\langle 56\rangle\langle 62\rangle\langle 5|1+6|2]} \tag{2.91}$$

Color-ordered tree amplitudes can exhibit physical poles only when the sum of momenta of adjacent external lines goes on-shell. As previously noted, MHV gluon amplitudes feature only

two-particle poles and do not possess multi-particle poles. In contrast, you have now seen that six-gluon NMHV amplitudes contain both two- and three-particle poles. Interestingly, in the BCFW representation, each diagram contributes a peculiar denominator factor of the form $\langle 5|1+6|2]$. This term does not correspond to any physical pole of the scattering amplitude—it is known as a ***spurious pole***. The residue associated with this unphysical pole must vanish, and indeed it does: the spurious contributions cancel out when summing over all relevant BCFW diagrams. More wisely, Hodges introduced the momentum twistor formalism to eliminate spurious poles [5] and the introduction of momentum twistors laid the foundation for the development of the amplituhedron [6], providing a natural coordinate system for its geometric formulation.

When does it work?

- Yang - Mills theory and gluon scattering.
- Scalar - QED.
- Scalar theory $\lambda\phi^4$.
- $\mathcal{N} = 4$ super Yang - Mills theory.
- Gravity.
- .....

3 (De)Constructed Gauge Theory

3.1 Motivation

Our four-dimensional description of spacetime may only be an effective low-energy approximation. While the observable universe appears four-dimensional — with one time and three spatial directions — it is possible that additional spatial dimensions exist but are hidden at quite small scales beyond our current experimental realm. A simple and widely reasearched realization of this thought involves compact extra dimensions, where fields propagate on a higher-dimensional spacetime with some dimensions compactified to small radius. At energies much lower than the compactification scale, such theories reduce to four-dimensional physics as an effetive theory, but at higher energies, the influence of these extra dimensions become manifest, for example, the appearance of Kaluza - Klein excitations(KK modes).

Theoretical interest in extra dimensions arises not only from string theory but also from the desire to better understand the ultraviolet behavior of field theories. Unfortunately, traditional higher-dimensional field theories are nonrenormalizable and contain dimensionful couplings, requiring a cutoff and becoming strongly coupled in the UV. This poses a major obstacle to fully understanding their high-energy behavior.

In response to this, Arkani-Hamed, Cohen, and Georgi proposed the idea of (De)constructed dimensions, in which higher-dimensional behavior emerges dynamically from a renormalizable four-dimensional theory. Their construction discretizes the extra dimension using a chain of gauge groups and link fields, producing a low-energy spectrum that mimics a compactified fifth dimension. Crucially, the theory remains perturbative and controllable in the UV, making it an ideal framework to study phenomena associated with extra dimensions—such as KK mode scattering—without running into the usual ultraviolet issues.

This paper is motivated by this (De)constructed approach. We focus on computing tree-level scattering amplitudes in the simplest two-site model, employing modern amplitude techniques such as the BCFW recursion relation, spinor-helicity formalism, and color ordering.

3.2 $SU(m) \times SU(n)$ *Moose*

At first, we consider four-dimensional field theories that contain gauge fields and fermions. These theories can be conveniently illustrated using a type of diagram known as a "moose" or "quiver" diagram[4]. In such diagrams, gauge groups are represented by open circles, and fermions are shown as single arrows (directed lines) attached to those circles.

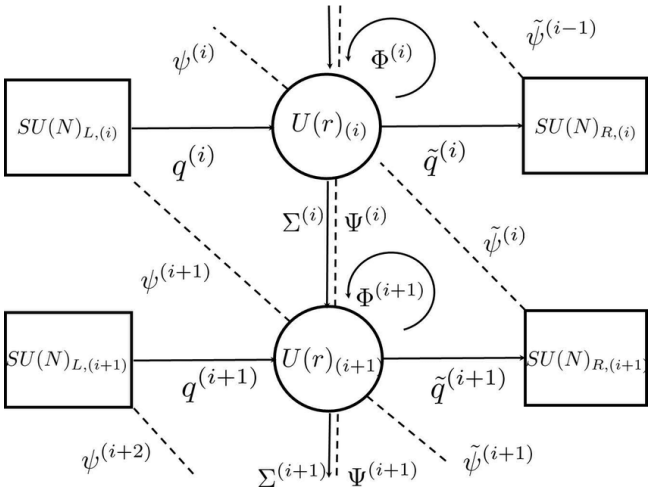

Figure 3: Example of quiver diagram

An arrow pointing away from a circle represents a set of Weyl fermions transforming under the fundamental representation of that gauge group. Conversely, an arrow pointing toward a circle corresponds to fermions transforming in the complex conjugate of fundamental representation.

We will focus on a specific example: a moose diagram shaped like an N-sided polygon, where each node and connection encodes the field content and gauge structure of the theory with gauge group $SU(m)^N \times SU(n)^N$

[4]Sorry for the ambiguity of different terminology. In this paper, the term "quiver", "moose" and "(De)construction" mainly represent the same meaning

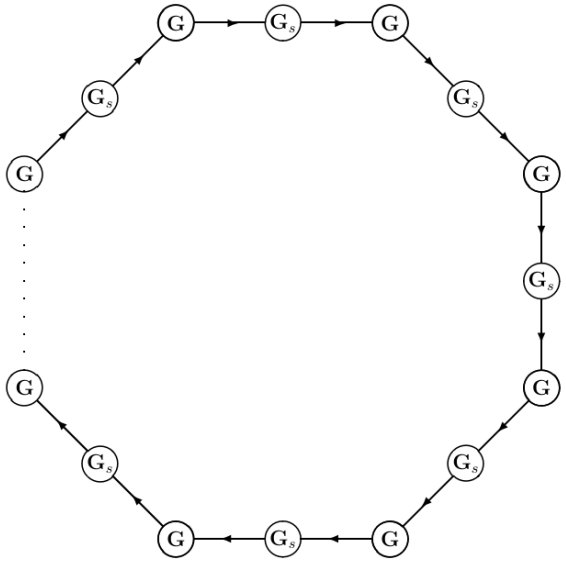

Figure 4: Moose diagram

We impose a *cyclic symmetry* on the theory so that all $SU(m)$ gauge couplings are set equal to a common value g, and all $SU(n)$ gauge couplings are set equal to g_s. Through *dimensional transmutation*, the theory can equivalently be described by two corresponding *dimensionful parameters*, Λ and Λ_s, which characterize the strong coupling scales of the respective gauge groups.

Each *side of the polygon* in the moose diagram represents two types of fermions, each transforming under the three gauge groups associated with that side: $SU_i(m) \times SU_i(n) \times SU_{i+1}(m)$.

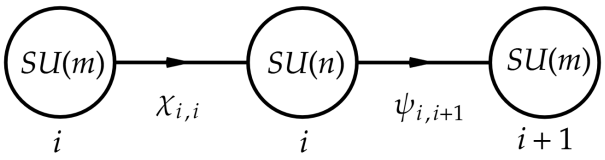

$$\chi_{i,i} \qquad \text{transformed under} \quad (m, \bar{n}, 1) \tag{3.1}$$

$$\psi_{i,i+1} \qquad \text{transformed under} \quad (1, n, \bar{m}) \tag{3.2}$$

where m, n refer to the fundamental representation of gauge group $SU(m)$ and $Su(n)$, $\bar{m}, \bar{n}$ refer to the conjugate of fundamental representation, and 1 just represent the trival representation.

Low-energy behavior. What does the theory look like at longer distances? In the regime where $\Lambda_s \gg \Lambda$, the low-energy behavior of the theory becomes relatively simple. At energy scales around Λ_s, the $SU(m)$ gauge couplings remain weak and can be treated

perturbatively. In contrast, each $SU(n)$ gauge group becomes strongly coupled at this scale, leading to ***fermion condensation***.

Specifically, pairs of fermions associated with each strong gauge group condense, forming nonzero vacuum expectation values:

$$\langle \chi_{i,i}\psi_{i,i+1}\rangle \sim 4\pi f^3\, U_{i,i+1}, \quad i = 1, \ldots, N$$

Here, $f \sim \Lambda_s/(4\pi)$ is the characteristic scale of the condensate, and $U_{i,i+1}$ is an $m \times m$ unitary matrix that encodes the orientation of the condensate in field space. And in thefollowing part, we will focus on the model after condensation.

We use a similar condensed - moose diagram to represent this condensed theory:

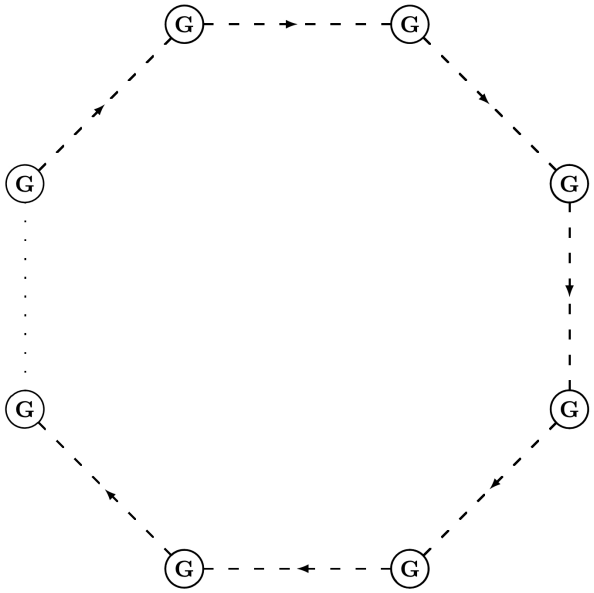

Figure 5: Condensed Moosed diagram

It is described by the following Lagrangian

$$\mathcal{L} = -\sum_{i=1}^{N} \frac{1}{2}\mathrm{Tr}(F_i)^2 + \sum_{i=1}^{N} \mathrm{Tr}[(D_\mu \Phi_i)^\dagger (D^\mu \Phi_i)], \tag{3.3}$$

here F_i refers to the ith gauge field strength, scalar field Φ_i transformed under the bi-fundamental representation and the covariant derivative equals to

$$D_\mu \Phi_i = \partial_\mu \Phi_i - i g_i A_{i\mu} \Phi_i + i g_{i+1} \Phi_i A_{i+1\mu}. \tag{3.4}$$

Here, gauge field and scalar field transformed like

$$\boldsymbol{A_{i\mu}} \to U_i(x) \boldsymbol{A_{i\mu}} U_i^-(x) - \frac{i}{g_i}(\partial_\mu U) U^{-1}, \qquad \Phi_i \to U_i(x) \Phi_i U_{i+1}^-(x) \tag{3.5}$$

It is easy to confirm that this theory is invariant under $\prod_1^N SU(m)$ gauge group.

The action is similar to the non-linear sigma model, in which the non-lenear sigma fields effectively connects gauge fields at neighboring sites. In fact, equation (3.3) can be interpreted as a discretized version of a five-dimensional gauge theory with gauge group $SU(m)$, where only the fifth dimension is latticized. The non-linear sigma model fields play the role of ***link variables*** in a lattice gauge theory, and the condensed moose diagram effectively represents the fifth dimension.

It is quite striking that the moose diagram, which was originally just a tool to keep track of fields and interactions in a four-dimensional theory, ***takes on a new physical meaning at low energies***: it effectively describes an extra spatial dimension.

We can higgs the scalar field $U_{i,i+1}$ making the gauge group down to the diagonal subgroup. Its eigenvalues can be easily computed, yielding a discrete mass spectrum labeled by an integer k satisfying $-N/2 < k \leq N/2$. The mass of each mode is given by:

$$M_k^2 = 4g^2 f_s^2 \sin^2\left(\frac{\pi k}{N}\right) \equiv \left(\frac{2}{a}\right)^2 \sin^2\left(\frac{p_5 a}{2}\right), \tag{3.6}$$

where $p_5 \equiv 2\pi k/R$ is the discretized momentum along the fifth dimension. The corresponding eigenvectors take the form $\psi^m \sim \exp(imp_5 a)$.

In the regime $|k| \ll N/2$, the spectrum becomes approximately linear, and the masses simplify to:

$$M_k \simeq |p_k| = \frac{2\pi|k|}{R}. \tag{3.7}$$

This exactly matches the ***Kaluza-Klein spectrum*** for a five-dimensional gauge boson compactified on a circle of circumference R. The effective four-dimensional gauge coupling of the diagonal subgroup is given by $g_4^2 = g^2/N$. Using the earlier relation in equation (2.7), this implies:

$$\frac{1}{g_4^2} = \frac{R}{g_5^2}, \tag{3.8}$$

which is the standard relation between the gauge couplings in five and four dimensions.

4 Scattering ampliyudes in 2 - site model

For simplicity, in this paper we only focus on the smallest block in this condensed moose theory – 2-site model, which can be represented by the following diagram

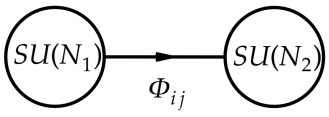

Figure 6: 2-site model

Here we choose a slightly different model, of which the two gauge group are different. The lagrangiian can be written like

$$\mathcal{L} = -\frac{1}{2}\mathrm{Tr}(F_1)^2 - \frac{1}{2}\mathrm{Tr}(F_2)^2 + \mathrm{Tr}[(D_\mu\Phi)^\dagger(D^\mu\Phi)], \tag{4.1}$$

The amplitudes are classified by their multiplicity:

3-point	4-point	5-point	6-point
$V_1\Phi\Phi^\dagger$	$V_1V_1V_1V_1$	$V_1V_1V_1V_1V_1$	$V_1V_1V_1V_1V_1V_1$
$V_2\Phi\Phi^\dagger$	$V_2V_2V_2V_2$	$V_2V_2V_2V_2V_2$	$V_2V_2V_2V_2V_2V_2$
$V_1V_1V_1$	$\Phi^\dagger V_1V_1\Phi$	$\Phi^\dagger V_1V_1V_1\Phi$	$\Phi^\dagger V_1V_1V_1V_1\Phi$
$V_2V_2V_2$	$\Phi V_2V_2\Phi^\dagger$	$\Phi V_2V_2V_2\Phi^\dagger$	$\Phi V_2V_2V_2V_2\Phi^\dagger$
	$\Phi V_2\Phi^\dagger V_1$	$V_2\Phi^\dagger V_1V_1\Phi$	$V_2V_2\Phi^\dagger V_1V_1\Phi$
	$\Phi\Phi^\dagger\Phi\Phi^\dagger$	$\Phi V_2V_2\Phi^\dagger V_1$	$\Phi V_2V_2\Phi^\dagger V_1V_1$
		$\Phi\Phi^\dagger\Phi\Phi^\dagger V_1$	$\vdots$
		$\Phi\Phi^\dagger\Phi\Phi^\dagger V_2$	$\vdots$

Table 1: Classification

4.1 3-point building block

We have known that the on-shell 3-point amplitudes can be completely determined by the little group scaling, according to the following formulas

$$A_3^{h_1h_2h_3} = c\langle 12\rangle^{h_3-h_1-h_2}\langle 31\rangle^{h_2-h_1-h_3}\langle 23\rangle^{h_1-h_2-h_3} \qquad h_1+h_2+h_3<0$$

$$A_3^{h_1h_2h_3} = c'[12]^{h_1+h_2-h_3}[23]^{h_2+h_3-h_1}[31]^{h_3+h_1-h_2} \qquad h_1+h_2+h_3>0$$

Because of the specialty of this kind of 2 site gauge theory, there are no direct interaction between gauge boson and scalar, so there are only two kinds of 3-point amplitudes.

- 2 scalar 1 gauge boson

$$A[1,2,3^+] = \frac{[23][31]}{[12]}, \qquad A[1,2,3^-] = \frac{\langle 23\rangle\langle 31\rangle}{\langle 12\rangle} \tag{4.2}$$

- 3 gauge boson

$$A[3^+,4^+,5^-] = \frac{[34]^3}{[45][53]}, \qquad A[3^-,4^-,5^+] = \frac{\langle 34\rangle^3}{\langle 45\rangle\langle 53\rangle} \tag{4.3}$$

If there are no exceptions, 1 and 2 always represent the scalar and antiscalar respectively, other number represent the gauge boson.

4.2 Gauge boson sector

In this section, we will show how to build the gauge boson scattering. Because there's no direct interaction between gauge boson 1 and gauge boson 2, so we only need to compute one of them. And although we have already known the formulas for MHV color-ordered amplitudes for gluon scattering – Parke-Talyor Formula

$$A[\cdots, i^-, \cdots, j^-, \cdots] = \frac{\langle ij\rangle^4}{\langle 12\rangle\langle 23\rangle\cdots\langle n-1,n\rangle\langle n1\rangle} \tag{4.4}$$

also for the anti-MHV amplitudes

$$A[\cdots, i^+, \cdots, j^+, \cdots] = \frac{[ij]^4}{[12][34]\cdots[n-1,n][n1]} \tag{4.5}$$

Here, we will give an concrete example to show how to use BCFW to compute the 4-point amplitudes $A[3^+, 4^+, 5^-, 6^-]$

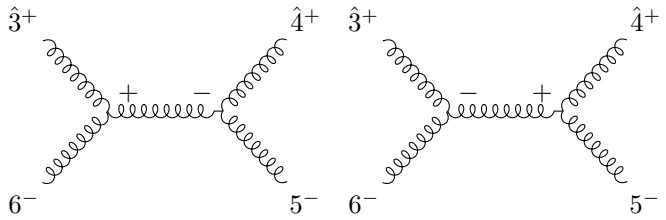

Figure 7: 4pt gluon

We choose the $[3,4\rangle$ shift, and it has been proved that $[+,+\rangle$ shift is valid

$$\begin{aligned} |\hat{3}] &= |3] - z|4], \qquad & |\hat{4}\rangle &= |4\rangle + z|3\rangle \\ |\hat{3}\rangle &= |3\rangle, & |\hat{4}] &= |4]. \end{aligned} \tag{4.6}$$

The first diagram can be evaluated

$$A_1 = \frac{[\hat{3}\hat{I}]^3}{[\hat{I}6][6\hat{3}]} \times \frac{1}{s_{36}} \times \frac{\langle 5\hat{I}\rangle^3}{\langle \hat{I}\hat{4}\rangle\langle \hat{4}5\rangle} \tag{4.7}$$

The point here is that

$$\text{Pole position}: \quad \hat{P}_{34}^2 = 0 = \langle 36\rangle[6\hat{3}] \quad \Rightarrow \quad [6\hat{3}] = 0, \tag{4.8}$$

for the similar reason, we can obtain $[\hat{I}6] = [6\hat{3}] = 0$, so we conclude that the left part

$$\frac{[\hat{3}\hat{I}]^3}{[\hat{I}6][6\hat{3}]} = 0 \tag{4.9}$$

so the first channel is vanishing.

The second diagram can be similarly evaluated

$$\begin{aligned} A_2 &= \frac{\langle \hat{I}6\rangle^3}{\langle 6\hat{3}\rangle\langle \hat{3}\hat{I}\rangle} \times \frac{1}{s_{36}} \times \frac{[\hat{I}\hat{4}]^3}{[\hat{4}5][5\hat{I}]} \\ &= \frac{[34]^3}{[34][45][56][61]} \end{aligned} \tag{4.10}$$

From this, we can conclude that the color-ordered amplitude equals to

$$A[3^+, 4^+, 5^-, 6^-] = \frac{[34]^3}{[34][45][56][63]}. \tag{4.11}$$

and it can also be expressed by angle brackets interchangeably

$$A[3^+, 4^+, 5^-, 6^-] = \frac{\langle 56\rangle^3}{\langle 34\rangle\langle 45\rangle\langle 56\rangle\langle 63\rangle} \tag{4.12}$$

Then, 5-point , 6-point can be recursively computed by using BCFW recursion relation.

4.3 SQCD like sector

4.3.1 4-point case

First we explain the color decomposition in this sector by 4 point amplitude $\Phi^\dagger V_1 V_1 \Phi$

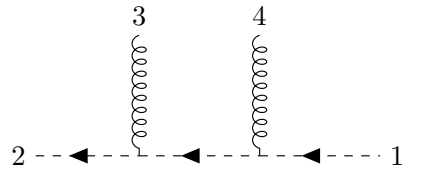

Figure 8: s channel

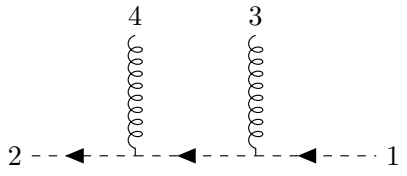

Figure 9: u channel

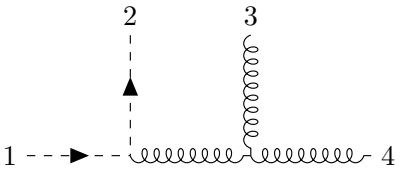

Figure 10: t channel

The color factor can be written respectively as following

$$r_s = \mathrm{Tr}[\Phi_2^\dagger T^{a_3} T^{a_4} \Phi_1], \quad r_u = \mathrm{Tr}[\Phi_2^\dagger T^{a_4} T^{a_3} \Phi_1], \quad r_t = \mathrm{Tr}[\Phi_2^\dagger [T^{a_3}, T^{a_4}] \Phi_1]$$

We can easily obtain a similar Jacobbi relation

$$r_t = r_s - r_u \tag{4.13}$$

Then we can accomplish the color decomposition and define the corressponding color-ordered amplitudes.

For example, in the 4pt. case, the full amplitude can be decomposed to the following form

$$\begin{aligned}\mathcal{A}_4(\Phi^\dagger V_1 V_1 \Phi) &= A_s r_s + A_u r_u + A_t r_t \\ &= A_s r_s + A_u r_u + A_t(r_s - r_u) \\ &= (A_s + A_t) r_s + (A_u - A_t) r_u \end{aligned} \tag{4.14}$$

The two subamplitudes can be defined as color-ordered amplitude with order [1,2,3,4] and [1,2,4,3] respectively. Of course, for the type $\Phi^\dagger(nV_1)\Phi$ and $\Phi(nV_2)\Phi^\dagger$, we can do the same thing to define the color-ordered amplitudes.

If there is no special case, we always choose the following BCFW shift

$$\begin{aligned} |\hat{2}] = |2] - z|3], \qquad & |\hat{3}\rangle = |3\rangle + z|3\rangle \\ |\hat{2}\rangle = |2\rangle, \qquad & |\hat{3}] = |3] \end{aligned} \tag{4.15}$$

where 2 always refers to antiscalar and 3 refers to gauge boson with + helicity.

We start from the 4-point color-ordered $A[1,2,3^+,4^-]$ again

$$A[1,2,3^+,4^-] = \sum_h$$

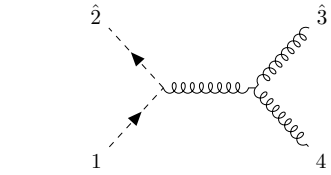

$$=$$

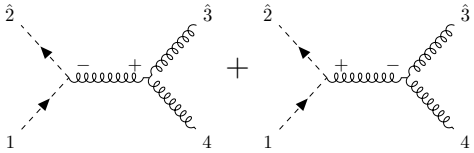

For the same reason, the contribution from the second diagram is vanishing, so we only need to compute the firt one

$$\begin{aligned} A_1 &= \frac{\langle \hat{2}\hat{I}\rangle\langle \hat{I}1\rangle}{\langle 1\hat{I}\rangle} \times \frac{1}{s_{12}} \times \frac{[\hat{I}\hat{3}]^3}{[\hat{3}4][4\hat{I}]} \\ &= (-1)\frac{\langle 14\rangle^2\langle 24\rangle^2}{\langle 12\rangle\langle 23\rangle\langle 34\rangle\langle 41\rangle} \end{aligned} \tag{4.16}$$

where we use the fact $|\hat{2}\rangle = |2\rangle$, $|\hat{3}] = |3]$, and the Fierz Identity

$$[ij][kl] + [il][jk] + [ik][lj] = 0 \tag{4.17}$$

Here we can prove a nonus relation $A[1,2,3^+,4^+] = 0$. Because of the vanishing of 3 gluon amplitude $A[+,+,+]$, so we only have one channel

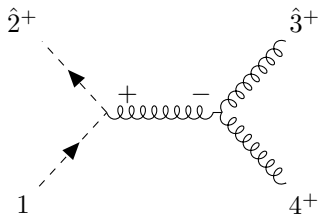

Figure 11: All plus

Similarly, beacuse of the on-shell pole, we obtain

$$[\hat{2}\hat{I}] = [\hat{I}1] = [1\hat{2}] = 0, \tag{4.18}$$

so the contribution from the left part

$$\frac{[\hat{2}\hat{I}][\hat{I}1]}{[1\hat{2}]} = 0, \tag{4.19}$$

then we can conclude that

$$A[1, 2, 3^+, 4^+] = 0 \tag{4.20}$$

4.3.2 5-point case

Still, from the 4-point amplitude, we can first obtain

$$A[1, 2, 3^+, 4^+, 5^+] = 0. \tag{4.21}$$

For the 5-point MHV case, here we only consider the $(+, +, -)$ case.

$A[1, 2, 3^+, 4^+, 5^+] =$

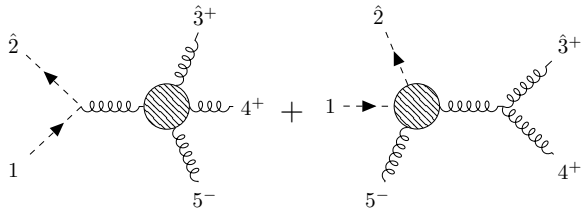

$$= 0 + \frac{\langle 2\hat{5}\rangle^2\langle 15\rangle}{\langle 12\rangle\langle 2\hat{I}\rangle\langle \hat{I}5\rangle} \times \frac{1}{s_{34}} \times \frac{[\hat{3}4]^3}{[4\hat{I}][\hat{I}3]} \tag{4.22}$$

then we use

$$\langle 2\hat{I}\rangle[\hat{I}3] = \langle 24\rangle[43], \quad [4\hat{I}]\langle \hat{I}5\rangle = [43]\langle \hat{3}5\rangle \tag{4.23}$$

from the pole position

$$\hat{P}_{34}^2 = 0 = \langle \hat{3}4\rangle[43] \quad \Rightarrow \quad \langle \hat{3}4\rangle = 0 \tag{4.24}$$

$$\langle 34\rangle + z\langle 24\rangle = 0 \quad \Rightarrow \quad z = -\frac{\langle 34\rangle}{\langle 24\rangle} \tag{4.25}$$

so

$$\langle \hat{3}5\rangle = \frac{\langle 32\rangle\langle 54\rangle}{\langle 24\rangle} \tag{4.26}$$

Then the color-ordered amplitude equals to

$$A[1,2,3^+,4^+,5^-] = \frac{\langle 15\rangle^2\langle 25\rangle^2}{\langle 12\rangle\langle 23\rangle\langle 34\rangle\langle 45\rangle\langle 51\rangle} \tag{4.27}$$

4.3.3 6 - point case

Similarly, we can obtain all - plus(minus) amplitude equals to 0

$$A_6[1,2,3^+,4^+,5^+,6^+] = A_6[1,2,3^-,4^-,5^-,6^-] = 0. \tag{4.28}$$

For the 6-point MHV amplitude $A_6[1,2,3^+,4^+,5^+,6^-]$, here are the corresponding diagrams

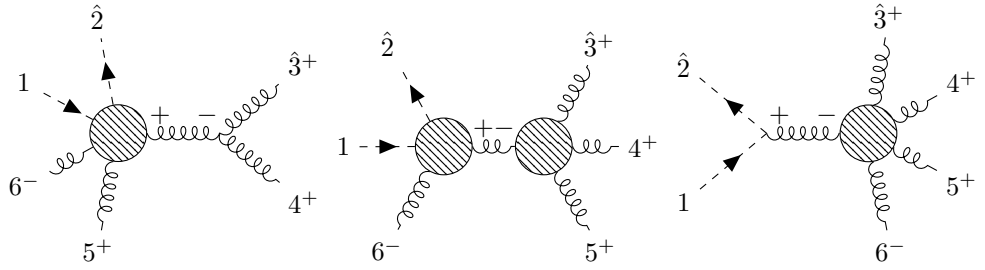

Figure 12: 6-point MHV

For the second diagram of Figure 12, there are pure gauge boson subamplitude $A_4[3^+,4^+,5^+,6^-] = 0$, so we conclude the second diagram gives vanishing contribution. For the third diagram,

$$\hat{P}_{12}^2 = 0 = 2p_1\cdot\hat{p}_2 = \langle 1\hat{2}\rangle[\hat{2}1] = \langle 12\rangle[\hat{2}1] = 0 \qquad \Rightarrow \qquad [\hat{2}1] = 0 \tag{4.29}$$

and similarly

$$[\hat{2}\hat{I}] = [1\hat{I}] = 0. \tag{4.30}$$

The third diagram equals to

$$A = \frac{[\hat{2}\hat{I}][\hat{I}]1}{[1\hat{2}]}\times\frac{1}{s_{12}}\times A_5[\hat{3}^+,4^+,5^+,6^-,\hat{I}^-] = 0. \tag{4.31}$$

The only non-vanishing comes from the first diagram equaling to

$$\begin{aligned} A &= \frac{\langle\hat{2}6\rangle^2\langle 61\rangle^2}{\langle 1\hat{2}\rangle\langle\hat{2}\hat{I}\rangle\langle\hat{I}5\rangle\langle 56\rangle\langle 61\rangle}\times\frac{1}{s_{34}}\times\frac{[\hat{3}4]^3}{[4\hat{I}][\hat{I}3]} \\ &= \frac{\langle 26\rangle^2\langle 61\rangle}{\langle 12\rangle\langle 2\hat{I}\rangle\langle\hat{I}5\rangle\langle 56\rangle}\times\frac{1}{s_{34}}\times\frac{[34]^3}{[4\hat{I}][\hat{I}]3} \end{aligned} \tag{4.32}$$

and we have the following equalities

$$\langle 2\hat{I}\rangle[\hat{I}3] + \langle 24\rangle[43], \qquad [4\hat{I}]\langle\hat{I}5\rangle = [43]\langle\hat{3}5\rangle \tag{4.33}$$

$\langle\hat{3}5\rangle$ can be obtained from the on-shell propagator

$$\hat{P}_{34}^2 = 0 = \langle\hat{3}4\rangle[4\hat{3}] = \langle\hat{3}4\rangle[43] \qquad \Rightarrow \qquad \langle\hat{3}4\rangle = 0, \tag{4.34}$$

then it can be derived that

$$\langle\hat{3}5\rangle = \frac{\langle 23\rangle\langle 45\rangle}{\langle 24\rangle}. \tag{4.35}$$

Finally, we can conclude that

$$\begin{aligned} A_6[1,2,3^+,4^+,5^+,6^-] &= \frac{\langle 26\rangle^2\langle 61\rangle\cancel{[34]^3\langle 24\rangle}}{\langle 12\rangle\langle 56\rangle\cancel{\langle 24\rangle[43][43]}\langle 23\rangle\langle 45\rangle\cancel{[34]}\langle 43\rangle} \\ &= (-1)\frac{\langle 26\rangle^2\langle 61\rangle^2}{\langle 12\rangle\langle 23\rangle\langle 34\rangle\langle 45\rangle\langle 56\rangle\langle 61\rangle}. \end{aligned} \tag{4.36}$$

Here, we need to notice that in 6-point case, we will first meet the NMHV amplitudes like $A_6[1,2,3^+,4^+,5^-,6^-]$. Although we can still compute it by samely utlizing BCFW recursion relaiton, but it is quite messy. So it is better to introduce another method named CSW expansion.

We introduce the general shift in section 2.4.1 like (2.61) and specialize to BCFW shift in section 2.4.2 like (2.71). Here, I will introduce another kind of recursion relation. Consider a shift which is implemented by a "holomorphic" square spinor shift:

$$|\hat{i}] = |i] + zc_i|X], \qquad |i\rangle = |i\rangle, \tag{4.37}$$

Here $|X]$ is an arbitrary reference spinor and the coefficients c_i satisfy $\sum_{i=1}^n c_i|i\rangle = 0$. Notice that this equation can be always solved and the shift spinors also satisfy momentum conservation and on-shell condition.

We consider here a situation where all $c_i \neq 0$ so that all momentum lines are shifted via(4.37) – this is an all-line shift. And the large - z behavior of all-line shift can be found in this paper [7]. As shown in [8], N^{K}MHV gluon tree amplitudes fall off as $1/z^K$ under an all-line shift in the large-z limit. This implies that all tree-level gluon amplitudes—except the MHV case with $K = 0$—can be fully constructed using the all-line shift recursion relations.

The critical point here is that the MHV amplitudes depend only on angle spinors, so the only way we can know about the square-spinor shift is arrording to the internal line angle spinors $|\hat{P}_I\rangle$, and this $|\hat{P}_I\rangle$ can be written in a wise manner

$$|\hat{P}_I\rangle\frac{[\hat{P}_I X]}{[\hat{P}_I X]} = \hat{P}_I|X]\frac{1}{[\hat{P}_I X]} = P_I|X]\frac{1}{[\hat{P}_I X]}, \tag{4.38}$$

where we can drop the hat upon the shifted momentum $\hat{P}_I$ because the shift is proportional to $|X]$, so that it will become 0 when contracting with itself. And other point is there are same number of $|P\rangle_I$ appearing in the numerator and demoninator as there's no helicity dependence on internal propagator, so that all of $\frac{1}{[\hat{P}_I X]}$ can be canceled with other.

Then for each diagram we can use the following prescription

$$|P\rangle_I \quad \to \quad P_I|X], \tag{4.39}$$

For example

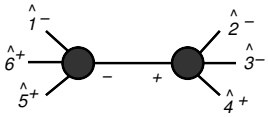

$$= \frac{\langle 1|P_{156}|X]^4}{\langle 1|P_{156}|X]\langle 5|P_{156}|X]\langle 56\rangle\langle 61\rangle} \cdot \frac{1}{P_{156}^2} \cdot \frac{\langle 23\rangle^4}{\langle 23\rangle\langle 34\rangle\langle 4|P_{156}|X]\langle 2|P_{156}|X]} \tag{4.40}$$

Here, for the 6-point amplitude $A_6[1,2,3^+,4^-,5^+,6^-]$, we can computing by this method

$$\begin{aligned} A_6[1,2,3^+,4^-,5^+,6^-] =& \frac{\langle 24\rangle^2\langle 4|P_{234}|X]}{\langle 2|P_{234}|X]\langle 23\rangle\langle 34\rangle} \times \frac{1}{s_{12}} \times \frac{\langle 6|P_{156}|x]^2\langle 61\rangle}{\langle 1|P_{156}|x]\langle 25\rangle\langle 56\rangle} \\ &+ \frac{\langle 24\rangle^2\langle 4|P_{61}|X]^2}{\langle 5|P_{61}|X]\langle 2|P_{61}|X]\langle 23\rangle\langle 34\rangle\langle 45\rangle} \times \frac{1}{s_{61}} \times \frac{\langle 61\rangle\langle 6|P_{61}|X]}{\langle 1|P_{61}|X]} \\ &+ \frac{\langle 1|P_{123}|X]^2\langle 2|P_{123}|X]}{\langle 3|P_{123}|X]\langle 13\rangle\langle 21\rangle} \times \frac{1}{s_{123}} \times \frac{\langle 46\rangle^4}{\langle 4|P_{456}|X]\langle 6|P_{456}|X]\langle 45\rangle\langle 56\rangle} \\ &+ \frac{\langle 14\rangle^2\langle 24\rangle^2}{\langle 4|P_{56}|X]\langle 1|P_{56}|X]\langle 23\rangle\langle 34\rangle} \times \frac{1}{s_{56}} \times \frac{\langle 6|P_{56}|X]^3}{\langle 5|P_{56}|X]\langle 56\rangle} \end{aligned} \tag{4.41}$$

In principle, there is another diagram contributing to this amplitude

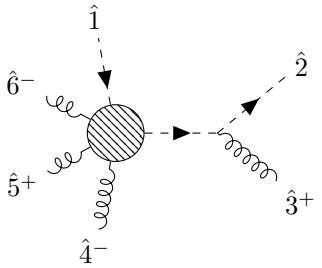

Figure 13: MHV × anti-MHV

but because of the 3 particle special kinematics, the 3-point anti-MHV part gives vanishing contributtion, this diagram actually equals to 0. This is why we called this method MHV expansion in the following.

In general, individual diagrams exhibit an explicit dependence on the reference spinor $|X]$. However, the full tree-level amplitude must remain independent of this arbitrary choice.The expansion of amplitudes using MHV vertex diagrams extends naturally beyond the NMHV level. More generally, an N^KMHV tree-level amplitude can be expressed as a sum over all

tree diagrams containing exactly $K+1$ MHV vertices. Henceforth, this method is called ***MHV vertex expansion***. But actually, this method was discovered by Cachazo, Svrcek, and Witten [9] befor introducing complex shift, so it is also named ***CSW expansion***.

4.3.4 n-point case

It is not so hard to generallize these results to general case, here we only provide the compact formula, and the negligible sign are neglected

$$A[1,2,\cdots,n^-] = \frac{\langle 1n\rangle^2\langle 2n\rangle^2}{\langle 12\rangle\langle 23\rangle\cdots\langle n-1,1\rangle\langle n,1\rangle}$$

4.4 Pure 2-site sector

4.4.1 4-point case

The color structure for this kind of amplitude has special form, like

$$(T_1^{a_1}T_1^{a_2}\cdots T_1^{a_{n_1}})_{ij}(T_2^{b_1}T_2^{b_2}\cdots T_2^{b_{n_2}})_{\bar{j}\bar{i}} \tag{4.42}$$

Here we start from the 4-point case with the color factor

$$(T_1^a)_{ij}(T_2^b)_{\bar{j}\bar{i}} \tag{4.43}$$

It is more straightforward to observe the color structure in terms of double line notation as follows

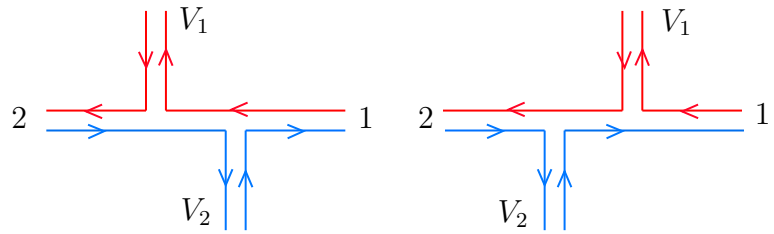

For the 4-point case $\mathcal{A}(V_2\Phi^\dagger V_1\Phi)$, we can construct the color-ordered amplitude from the residue. First, we consider the $(+,-)$ helicity configuration. There are two feynman diagrams contributing to the color-ordered amplitude.

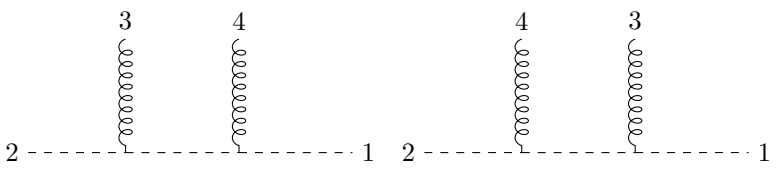

Figure 14: 4pt.

Because we choose $[2,3\rangle$ shift here, so there is only one valid BCFW channel

$$\begin{aligned} A[1,2,3_1^+,4_2^-] &= \frac{\langle\hat{2}4\rangle\langle 4\hat{I}\rangle}{\langle\hat{I}\hat{2}\rangle}\times\frac{1}{s_{24}}\times\frac{[\hat{I}\hat{3}][\hat{3}1]}{[1\hat{I}]} \\ &= \frac{[13][23]}{[14][24]} \end{aligned}$$

it seems that this amplitude is different from others before, because it is expressed solely in terms of angle brackets, but of course it can be rewritten to another form.

$$\begin{aligned} \frac{[13][23]}{[14][24]} &= \frac{\langle 23\rangle[31]}{\langle 23\rangle[41]}\times\frac{[23]\langle 31\rangle}{[24]\langle 31\rangle} \\ &= -\frac{\langle 24\rangle\cancel{[41]}}{\langle 23\rangle\cancel{[41]}}\times(-1)\frac{\cancel{[24]}\langle 41\rangle}{\cancel{[24]}\langle 31\rangle} \\ &= \frac{\langle 14\rangle\langle 24\rangle}{\langle 13\rangle\langle 23\rangle} \end{aligned}$$

Also, we can compute it from direct gluing. For the first diagram, the residue equals to

$$\text{Res}|_{s_{12}=0} = \frac{[3I][23]}{[I2]}\times\frac{\langle I4\rangle\langle 41\rangle}{\langle 1I\rangle} = \frac{\langle 24\rangle[31]\langle 41\rangle[23]}{[42]\langle 24\rangle}$$

Similarly, the second one is

$$\text{Res}|_{s_{13}=0} = \frac{\langle 4I\rangle\langle 24\rangle}{\langle I2\rangle}\times\frac{[31][I3]}{[1I]} = \frac{\langle 24\rangle[31]\langle 41\rangle[23]}{\langle 32\rangle[23]}$$

Then we can conclude that the four-point color-ordered amplitude $A[1,2,3^+,4^-]$ equals to

$$A[1,2,3^+,4^-] = \frac{\langle 24\rangle[31]\langle 41\rangle[23]}{\langle 32\rangle[23][42]\langle 24\rangle} = \frac{\langle 24\rangle\langle 14\rangle}{\langle 13\rangle\langle 23\rangle}$$

⋆Bonus

It is still necessary to prove the color-ordered amplitude $A[1,2,3^+,4^+]$ equals to 0. Here we can use the color ordered Feynman rules to show the result.

$$A[1,2,3^+,4^+] \propto \frac{(\epsilon_3\cdot p_2)\,(\epsilon_4\cdot p_1)}{s_{23}} + \frac{(\epsilon_4\cdot p_2)\,(\epsilon_3\cdot p_1)}{s_{24}}$$

Here we can utilize the spinor-helicity variable to express polarization vector

$$\epsilon_2^{+\mu} = \frac{\langle r_1|\gamma^\mu|3]}{\sqrt{2}\langle r_1 3\rangle}, \qquad \epsilon_4^{+\mu} = \frac{\langle r_2|\gamma^\mu|4]}{\sqrt{2}\langle r_2 4\rangle}$$

here r_1 and r_2 represent the reference spinor.

We can freely choose $r_1 = r_2 = 1$ or 2, then $\langle r_1 2\rangle$,$\langle r_2 1\rangle$,$\langle r_1 1\rangle$,$\langle r_2 2\rangle$, two of them equal to 0,

so we can conclude that

$$A[1, 2, 3^+, 4^+] = 0$$

4.4.2 5-point case

For the 5-point case, we can utilize the BCFW recursion relation which can help us generate higher point amplitude from lower point on-shell subamplitudes. Here, we always consider the MHV (Maximal helicity violation) amplitude.

Let us begin with the simplest case $A[1, 2, 3_1^+, 4_1^+, 5_2^-]$, where the subscript represent which gauge group the particle belongs to. Because of the property of this kind of gauge theory, the color structure is invariant under the OPP (Order Preserving Permutation), in this case, for example,

$$(3_1^+, 4_1^+, 5_2^-) \qquad (3_1^+, 5_2^-, 4_1^+) \qquad (5_2^-, 3_1^+, 4_1^+) \tag{4.44}$$

give us the same color factor. So in the process of BCFW recursion, these three order offer the same amplitude. We can draw all diagrams contributing to the BCFW process, the first two are following

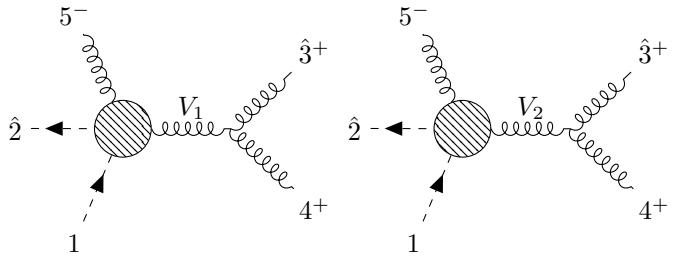

Figure 15: 5pt. 1

It is obvious that the second diagram in Figure 13 equals to 0, because there are no interaction between the two gauge bosons. Similarly, another two diagrams equal to 0 for the same reason

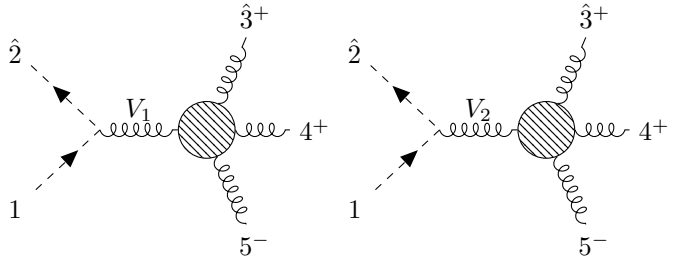

Figure 16: 5pt. 2

The last diagram still gives 0 contribution because it includes a subamplitude $A[1, \hat{I}, \hat{3}^+, 4^+] = 0$.

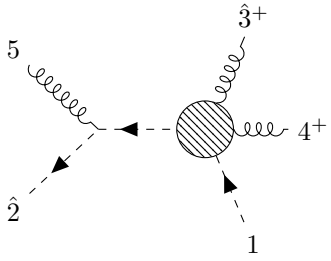

Figure 17: 5pt. 3

Above all. only the first diagram in Figure 1 has non-vanishing contributions, so the full color ordered amplitude equals to

$$\begin{aligned} A[1,2,3_1^+,4_1^+,5_2^-] &= A[1,2,\hat{I}^+,5^-] \times \frac{1}{s_{34}} \times A[\hat{3}^+,4^+,\hat{I}^-] \\ &= \frac{\langle 15\rangle\langle 25\rangle}{\langle 1\hat{I}\rangle\langle 2\hat{I}\rangle} \times \frac{1}{s_{34}} \times \frac{[\hat{3}4]^3}{[4\hat{I}][\hat{I}\hat{3}]} \\ &= \frac{\langle 15\rangle\langle 25\rangle\cancel{[34]^3}}{\langle 14\rangle\langle 23\rangle\langle 43\rangle\cancel{[43][43][34]}} \qquad (4.45) \\ &= \frac{\langle 15\rangle\langle 25\rangle}{\langle 23\rangle\langle 34\rangle\langle 41\rangle} \\ &= \frac{(-1)\langle 25\rangle^2\langle 15\rangle^2}{\langle 23\rangle\langle 34\rangle\langle 41\rangle\langle 25\rangle\langle 51\rangle} \qquad (4.46) \end{aligned}$$

where we use the fact $|\hat{3}\rangle = |\hat{3}\rangle$ and following identities

$$\langle 1\hat{I}\rangle[\hat{I}3] = \langle 14\rangle[43], \quad \langle 2\hat{I}\rangle[\hat{I}3] = \langle 24\rangle[43] \qquad (4.47)$$

and also

$$\begin{aligned} \frac{[\hat{I}3]}{[4\hat{I}]} &= -\frac{[3\hat{I}]\langle\hat{I}2\rangle}{[4\hat{I}]\langle\hat{I}2\rangle} = -\frac{[34]\langle 42\rangle}{[43]\langle\hat{3}2\rangle}, \quad (\langle\hat{3}2\rangle = \langle 32\rangle + z\langle 22\rangle = \langle 32\rangle) \\ &= \frac{\langle 42\rangle}{\langle 32\rangle} \qquad (4.48) \end{aligned}$$

here green refers to the particle with (-) helicity, red refers to particles belong to gauge group 1, red refers to particles belong to gauge group 2.

Similarly, it is very easy to obtain another color-ordered amplitude $A[1,2,3_1^+,4_1^-,5_2^+]$

$$A[1,2,3_1^+,4_1^-,5_2^+] = \frac{(-1)\langle 24\rangle^2\langle 14\rangle^2}{\langle 23\rangle\langle 34\rangle\langle 41\rangle\langle 25\rangle\langle 51\rangle} \qquad (4.49)$$

and also $A[1,2,3_1^-,4_1^+,5_2^+]$ equals to

$$A[1,2,3_1^-,4_1^+,5_2^+] = \frac{(-1)\langle 23\rangle^2\langle 13\rangle^2}{\langle 23\rangle\langle 34\rangle\langle 41\rangle\langle 25\rangle\langle 51\rangle} \tag{4.50}$$

But here we need to emphasize that it is necessary to choose another BCFW shift, like $[1,5^+\rangle$, as $[2,3^-\rangle$ is not a valid shift.

4.4.3 6-point case

Here we consider $(V_2V_2\Phi^\dagger V_1V_1\Phi)$ case, the corresponding color-ordered amplitude is $A[1,2,3_1^+,4_1^+,5_2^+,6_2^-$ Similarly, the fowwling orders all give us the same color factor

$$\begin{array}{lll} (3_1^+,4_1^+,5_2^+,6_2^-) & (3_1^+,5_2^+,4_1^+,6_2^-) & (3_1^+,5_2^+,6_2^-,4_1^+) \\ (5_2^+,3_1^+,4_1^+,6_2^-) & (5_2^+,3_1^+,6_2^-,4_1^+) & (5_2^+,6_2^-,3_1^+,4_1^+) \end{array} \tag{4.51}$$

Evey OPP corresponds different BCFW diagrams, here for concreteness, we list all of the diagrams as following

- $(3_1^+,4_1^+,5_2^+,6_2^-)$

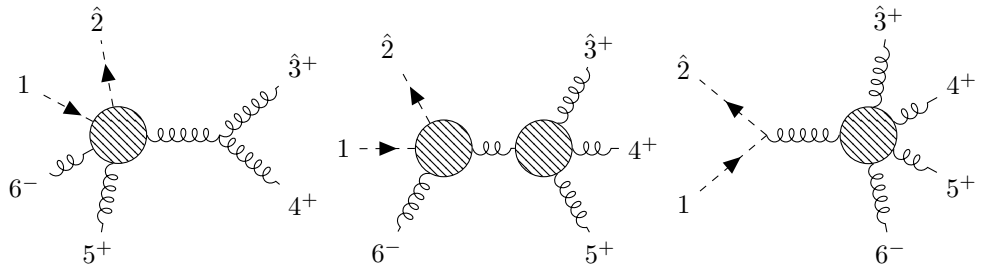

Figure 18: Order $(3_1^+,4_1^+,5_2^+,6_2^-)$

- $(3_1^+,5_2^+,4_1^+,6_2^-)$

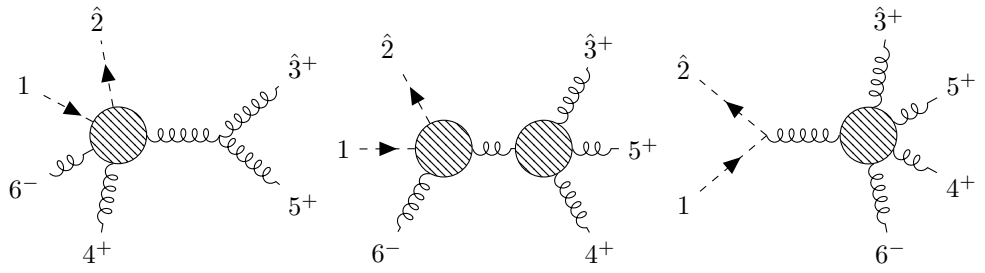

Figure 19: Order $(3_1^+,5_2^+,4_1^+,6_2^-$

- $(3_1^+,5_2^+,6_2^-,4_1^+)$

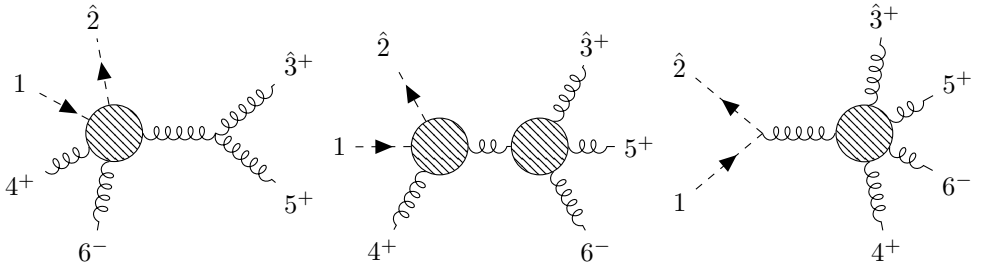

Figure 20: Order $(3_1^+, 5_2^+, 6_2^-, 4_1^+)$

- $(5_2^+, 3_1^+, 4_1^+, 6_2^-)$

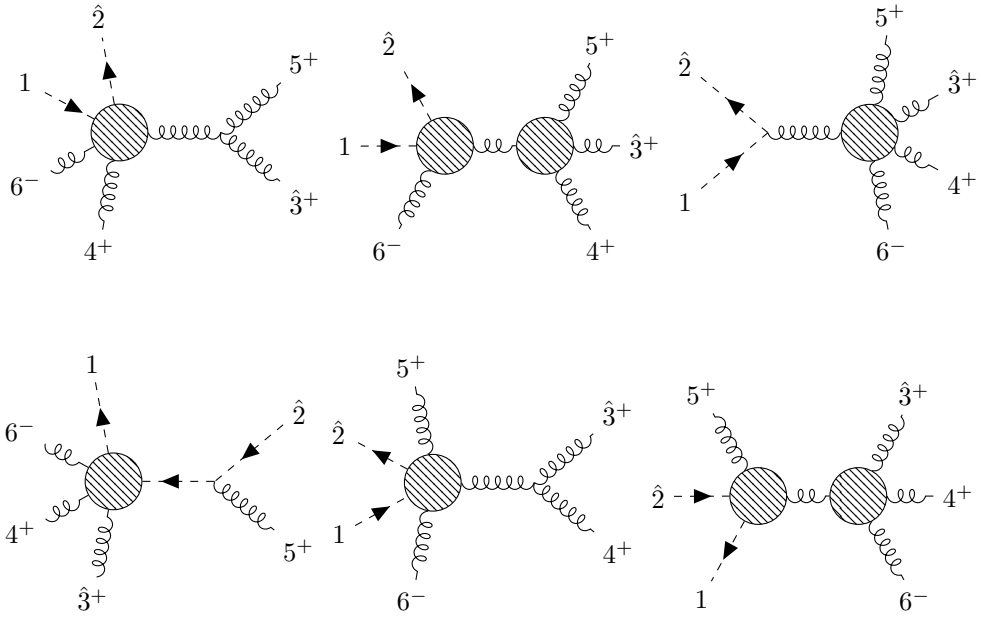

Figure 21: Order $(5_2^+, 3_1^+, 4_1^+, 6_2^-)$

- $(5_2^+, 3_1^+, 6_2^-, 4_1^+)$

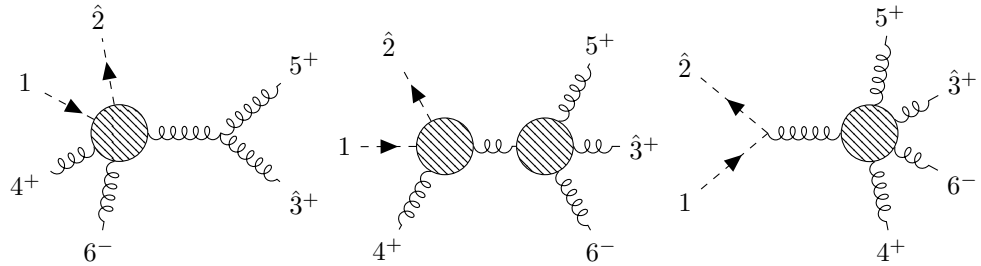

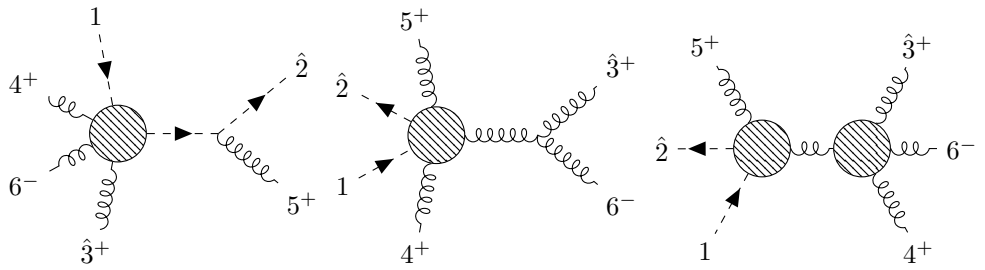

Figure 22: Oredr $(5_2^+, 3_1^+, 6_2^-, 4_1^+)$

- $(5_2^+, 6_2^-, 3_1^+, 4_1^+)$

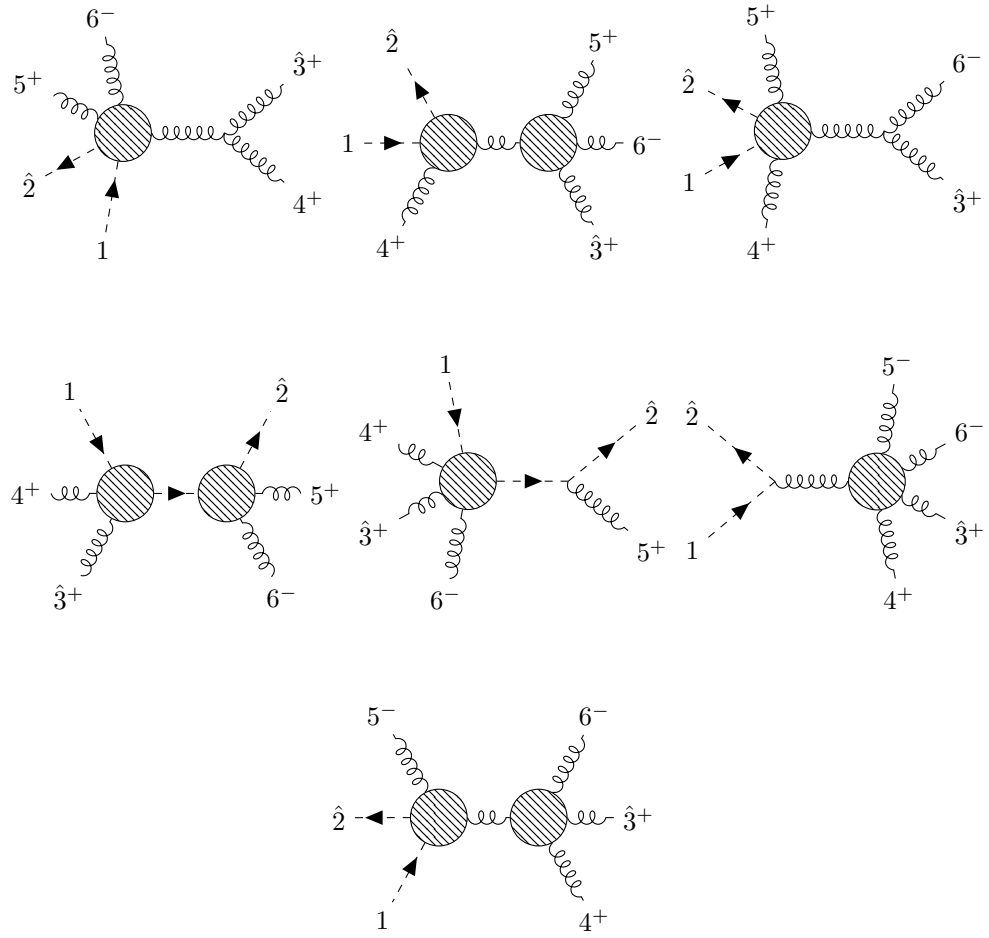

Figure 23: Order $(5_2^+, 6_2^-, 3_1^+, 4_1^+)$

Most of them equal to 0 because of there are no interaction between two gauge bosons or special helicity configuration. And some of the nonvanishing diagrams have same structure under OPP so they conly contribute once. Finally, only two diagrams have semmingly non-zero contribution,

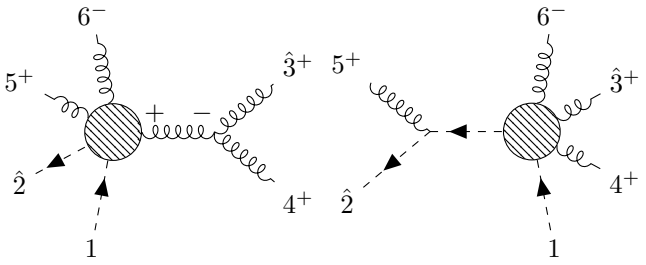

Figure 24: 6pt.

so the full color ordered amplitude equals to

$$\begin{aligned} A_1 &= \frac{(-1)\langle\hat{2}6\rangle^2\langle 16\rangle^2}{\langle 25\rangle\langle 56\rangle\langle 61\rangle\langle\hat{2}\hat{I}\rangle\langle\hat{I}1\rangle} \times \frac{1}{s_{34}} \times \frac{[\hat{3}4]^3}{[4\hat{I}][\hat{I}\hat{3}]} \\ &= \frac{\langle 26\rangle^2\langle 16\rangle}{\langle 25\rangle\langle 56\rangle\langle\hat{2}\hat{I}\rangle\langle\hat{I}1\rangle} \times \frac{1}{s_{34}} \times \frac{[34]^3}{[4\hat{I}][\hat{I}3]} \\ &= \frac{\langle 26\rangle^2\langle 16\rangle\cancel{[34]^3\langle 42\rangle}}{\langle 25\rangle\langle 56\rangle\langle 41\rangle\langle 32\rangle\langle 43\rangle\cancel{[43][43][34]\langle 24\rangle}} \\ &= \frac{\langle 26\rangle^2\langle 16\rangle^2}{\langle 23\rangle\langle 34\rangle\langle 41\rangle\langle 25\rangle\langle 56\rangle\langle 51\rangle} \end{aligned} \tag{4.52}$$

where we have used the fact $|\hat{2}\rangle = |2\rangle$, $|\hat{3}] = |3]$, and the following identities

$$\langle 2\hat{I}\rangle[\hat{I}3] = \langle 24\rangle[43], \qquad [4\hat{I}]\langle\hat{I}1\rangle = [43]\langle\hat{3}1\rangle \tag{4.53}$$

The point here is that we first $\langle\hat{3}1\rangle$ which does not appear in 5-point case, so we nned to compute it carefully

$$\begin{aligned} &\text{pole position}: \quad \hat{P_{34}}^2 = 0 = 2P_3 \cdot P_4 = \langle 4\hat{3}][34] \quad \Rightarrow \quad \langle 4\hat{3}\rangle = 0 \\ &\langle 43\rangle + z\langle 42\rangle = 0 \quad \Rightarrow \quad z = -\frac{43}{42} \end{aligned} \tag{4.54}$$

then

$$\begin{aligned} \langle\hat{3}1\rangle = \langle 31\rangle + z\langle 21\rangle &= \langle 31\rangle - \frac{\langle 43\rangle}{\langle 42\rangle}\langle 21\rangle \\ &= \frac{\langle 42\rangle\langle 31\rangle - \langle 43\rangle\langle 21\rangle}{42} \\ &= \frac{\langle 41\rangle\langle 32\rangle}{\langle 42\rangle} \end{aligned} \tag{4.55}$$

where we have used the Fierz identity

$$\langle 42\rangle\langle 31\rangle + \langle 41\rangle\langle 23\rangle + \langle 43\rangle\langle 12\rangle = 0. \tag{4.56}$$

Simiraly, we can compute the second diagram

$$A_2 = \frac{[\hat{2}5][5\hat{I}]}{[\hat{I}\hat{2}]} \times \frac{1}{s_{25}} \times \frac{(-1)\langle 16\rangle^2 \langle \hat{I}6\rangle^2}{\langle \hat{I}\hat{3}\rangle\langle \hat{3}4\rangle\langle 41\rangle\langle \hat{I}6\rangle\langle 61\rangle} \tag{4.57}$$

but from the pole position

$$\hat{P_{25}}^2 = 0 = 2P_2 \cdot P_5 = \langle 52\rangle[\hat{2}5] \qquad \Rightarrow \qquad [\hat{2}5] = 0, \tag{4.58}$$

and simiraly

$$[\hat{2}\hat{I}] = [5\hat{I}] = 0. \tag{4.59}$$

Then we can conclude that the left part of the amplitude equals to 0 so $A_2 = 0$. Finally, we obtain the color-ordered amplitude

$$A[1, 2, 3_1^+, 4_1^+, 5_2^+, 6_2^-] = A_1 + A_2 = \frac{\langle 26\rangle^2\langle 16\rangle^2}{\langle 23\rangle\langle 34\rangle\langle 41\rangle\langle 25\rangle\langle 56\rangle\langle 51\rangle}. \tag{4.60}$$

For the NMHV ampitudes $A[1, 2, 3_1^+, 4_1^-, 5_2^+, 6_2^-]$, we can obtain the following equation

$$\begin{aligned} A[1, 2, 3_1^+, 4_1^-, 5_2^+, 6_2^-] =& \frac{\langle 24\rangle\langle 4|P_{234}|X]}{\langle 24\rangle\langle 3|P_{234}|X]} \times \frac{1}{s_{234}} \times \frac{\langle 61\rangle\langle 6|P_{156}|X]}{\langle 51\rangle\langle 5|P_{156}|X]} \\ &+ \frac{\langle 26\rangle\langle 6|P_{256}|X]}{\langle 25\rangle\langle 5|P_{256}|X]} \times \frac{1}{s_{256}} \times \frac{\langle 14\rangle\langle 4|P_{134}|X]}{\langle 13\rangle\langle 3|P_{134}|X]} \\ &+ \frac{\langle 26\rangle^2\langle 61\rangle}{\langle 25\rangle\langle 56\rangle\langle 2|P_{34}|X]\langle 1|P_{34}|X]} \times \frac{1}{s_{34}} \times \frac{\langle 4|P_{34}|X]^3}{\langle 34\rangle\langle 3|P_{34}|X]} \\ &+ \frac{\langle 24\rangle^2\langle 41\rangle}{\langle 23\rangle\langle 36\rangle\langle 2|P_{56}|X]\langle 1|P_{56}|X]} \times \frac{1}{s_{56}} \times \frac{\langle 6|P_{56}|X]^3}{\langle 56\rangle\langle 5|P_{56}|X]}. \end{aligned} \tag{4.61}$$

where I do not cancel the dependence of spinor X explicitly, but it is not quite complicated to do.

4.4.4 n-point case

Here, we first propose a compact formula for the color-ordered amplitude

$$A = \frac{\langle 2a\rangle^2\langle 1a\rangle^2}{\underbrace{\langle 2\star\rangle \cdots \langle \star 1\rangle}_{SU(N_1)} \underbrace{\langle 2*\rangle \cdots \langle *1\rangle}_{SU(N_2)}} \tag{4.62}$$

where a refer to the particle with - helicity, whichever gauge group it belongs to. And, '$\star$' refers to the ordering for the first gauge group, '$*$' refers to the ordering for the second gauge group. We suppose there are n_1 gauge boson 1, n_2 gauge boson 2, so the n-point means that $n = n_1 + n_2 + 2$.

The usual way to prove this kind of compact formula is induction. First we suppose that

all of the amplitudes with external point lower than n satisfy the compact formula.

4.5 Pure scalar case

Before going to the computation of pure scalar amplitudes in the 2-site model, it is necessary to review a quite similar amplitude – scalar QED. There are two feynman diagrams corresponding to 4 scalar scattering process

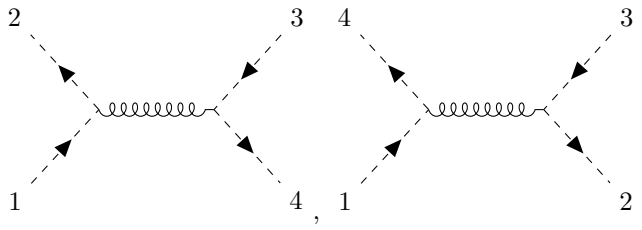

Figure 25: 4 scalar scattering

First we can use the feynman rule to compute them like

$$\begin{aligned} i\mathcal{A} &= (-ie)^2(-i) \times \frac{(p_1-p_2)(p_3-p_4)}{(p_1+p_2)^2} + (-ie)^2(-i)\frac{(p_1-p_4)(p_3-p_2)}{(p_1+p_4)^2} \\ &= ie^2\left(\frac{u-t}{s}+\frac{u-s}{t}\right) \\ &= -2ie^2 - 2ie^2\left(\frac{t}{s}+\frac{s}{t}\right) \end{aligned} \tag{4.63}$$

where the Mandelstam variables are defined as

$$s=(p_1+p_2)^2, \quad t=(p_1+p_4)^2, \quad u=(p_1+p_3)^2. \tag{4.64}$$

We can rewrite this formula in terms of spinor-helicity variables

$$s=\langle 12\rangle[21]=\langle 34\rangle[43], \quad t=\langle 14\rangle[41]=\langle 23\rangle[32], \quad u=\langle 13\rangle[31]=\langle 24\rangle[42]. \tag{4.65}$$

then the amplitudes can be rewritten like

$$\mathcal{A}=-2e^2-2e^2\left(\frac{\langle 14\rangle\langle 23\rangle}{\langle 12\rangle\langle 34\rangle}+\frac{\langle 12\rangle\langle 34\rangle}{\langle 14\rangle\langle 23\rangle}\right) \tag{4.66}$$

The second term can be written further as

$$\begin{aligned} \frac{\langle 14\rangle\langle 23\rangle}{\langle 12\rangle\langle 34\rangle}+\frac{\langle 12\rangle\langle 34\rangle}{\langle 14\rangle\langle 23\rangle} &= \frac{\langle 14\rangle^2\langle 23\rangle^2+\langle 12\rangle^2\langle 34\rangle^2}{\langle 14\rangle\langle 23\rangle\langle 12\rangle\langle 34\rangle} = \frac{(\langle 14\rangle\langle 23\rangle+\langle 12\rangle\langle 34\rangle)^2-2\langle 14\rangle\langle 23\rangle\langle 12\rangle\langle 34\rangle}{\langle 14\rangle\langle 23\rangle\langle 12\rangle\langle 34\rangle} \\ &= -\frac{\langle 13\rangle^2\langle 24\rangle^2}{\langle 12\rangle\langle 23\rangle\langle 34\rangle\langle 41\rangle}-2 \end{aligned} \tag{4.67}$$

then the final form of amplitudes can be read as

$$\mathcal{A} = \underbrace{2e^2}_{\text{boundary term}} + 2e^2 \frac{\langle 13\rangle^2 \langle 24\rangle^2}{\langle 12\rangle\langle 23\rangle\langle 34\rangle\langle 41\rangle} \tag{4.68}$$

where the meaning of boundary term can be understood later.

If we use BCFW to compute the same amplitude, can we obtain the same result? We choose the normal $[1,3\rangle$ shift and it corresponds two following BCFW channel

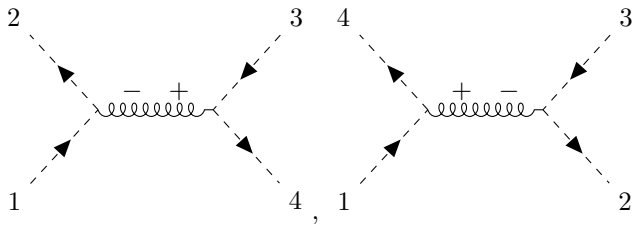

It can be computed like

$$\begin{aligned}
\mathcal{A} &= \frac{\langle \hat{1}\hat{I}\rangle\langle \hat{I}2\rangle}{\langle \hat{1}2\rangle} \times \frac{1}{s_{12}} \times \frac{[4\hat{I}][\hat{I}3]}{[\hat{3}4]} + \frac{\langle \hat{1}\hat{I}\rangle\langle \hat{I}4\rangle}{\langle 4\hat{1}\rangle} \times \frac{1}{s_{14}} \times \frac{[\hat{3}\hat{I}][\hat{I}2]}{[2\hat{3}]} \\
&= \frac{\langle 13\rangle\langle 24\rangle}{\langle 14\rangle\langle 23\rangle} + \frac{\langle 13\rangle\langle 24\rangle}{\langle 12\rangle\langle 34\rangle} \\
&= (-1)g^2 \frac{\langle 13\rangle^2\langle 24\rangle^2}{\langle 12\rangle\langle 23\rangle\langle 34\rangle\langle 41\rangle}
\end{aligned} \tag{4.69}$$

so if we choose $g = \sqrt{2}e$, we can notice that BCFW actually reproduce partial part of the full amplitude.If we compute the large-z behavior for equation (4.68), we can find that

$$\mathcal{A}|_{z\to\infty} = 2e^2 \tag{4.70}$$

this is why we called it boundary term before. More geneally, if we consider a sclar QED action including a ϕ^4 term like

$$\begin{aligned}
\mathcal{L} &= -\frac{1}{4}F_{\mu\nu}F^{\mu\nu} - |D\varphi|^2 - \frac{1}{4}\lambda|\varphi|^4 \\
&= -\frac{1}{4}F_{\mu\nu}F^{\mu\nu} - |\partial_\mu\varphi|^2 + ieA^\mu\left[(\partial_\mu\varphi^*)\varphi - \varphi^*\partial_\mu\varphi\right] - e^2A^\mu A_\mu\varphi^*\varphi - \frac{1}{4}\lambda|\varphi|^4
\end{aligned} \tag{4.71}$$

The 4-pt amplitude can be computed like

$$A_4(\varphi\,\varphi^*\varphi\,\varphi^*) \;=\; -\lambda + \tilde{e}^2\left(1 + \frac{\langle 13\rangle^2\langle 24\rangle^2}{\langle 12\rangle\langle 23\rangle\langle 34\rangle\langle 41\rangle}\right), \tag{4.72}$$

so actually we compute ta special case in which the parameter λ are choosed as $\lambda = 2e^2$, so that the boundary are eliminated.

Similarly, if we consider four sclar scattering in 2-site model $\Phi\Phi^\dagger\Phi\Phi^\dagger$, we have the same Feynman diagram but with two different gauge boson propagating in the internal line

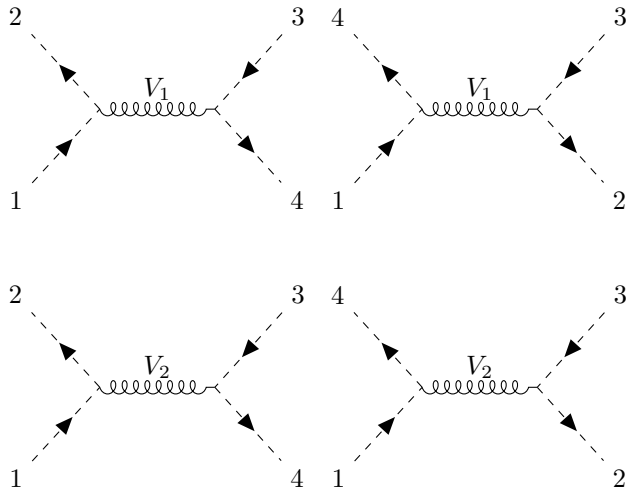

These diagrams correspond to two different amplitudes

$$\begin{aligned}\mathcal{A}_1 &= g_1^2\left(\frac{-2t-s}{s}\right)r_s + g_1^2\left(\frac{-2s-t}{t}\right)r_t \\ &= g_1^2\left(-1-2\frac{t}{s}\right)r_s + g_1^2\left(-1-2\frac{s}{t}\right)r_t \\ &= -g_1^2(r_s+r_t) - 2g_1^2\left(\frac{t}{s}r_s + \frac{s}{t}r_t\right)\end{aligned} \tag{4.73}$$

4.6 Attempt to massive scalar

It is quite intriguing to investigate what is the situation if we change the scalar to be massive. Without doubt, the BCFW shift should change and here we just refer to the method from [10]. The shift are choosen like

$$|\hat{2^I}\rangle = |2^I\rangle, \qquad |\hat{2^I}] = |2^I] - \frac{z}{m}|3][2^I3] \tag{4.74}$$

$$|\hat{3}\rangle = |3\rangle + \frac{z}{m}p_2|3], \qquad |\hat{3}] = |3]. \tag{4.75}$$

For the massive particle with same mass, it is necessary to introduce a x factor as [11]. Here the x factor equals to

$$x\lambda_{3\alpha} = \frac{p_{1\alpha\dot{\alpha}}}{m}\tilde{\lambda}_3^{\dot{\alpha}} \quad \Rightarrow \quad x\langle\xi 3\rangle = \frac{\langle\xi|p_1|3]}{m} \qquad x = \frac{\langle\xi|p_1|3]}{m\langle\xi 3\rangle} \tag{4.76}$$

$$\frac{\tilde{\lambda}_3^{\dot{\alpha}}}{x} = \frac{p_1^{\alpha\dot{\alpha}}\lambda_{3\alpha}}{m} \quad \Rightarrow \quad \frac{1}{x}[\xi 3] = \frac{\langle 3|p_1|\xi]}{m} \qquad \frac{1}{x} = \frac{\langle 3|p_1|\xi]}{m[3\xi]} \text{ or } x = \frac{m[\xi 3]}{\langle 3|p_1|\xi]} \tag{4.77}$$

Then, from the 3-point building block

$$M^{\text{min,+1}} = x\frac{\langle\mathbf{12}\rangle^{2s}}{m^{2s-1}}, \qquad M^{\text{min,-1}} = \frac{1}{x}\frac{[\mathbf{12}]^{2s}}{m^{2s-1}} \tag{4.78}$$

here min means the minimal coupling. The amplitudes can be similarly computed by utlizing BCFW with some more efforts

$$\begin{aligned} A[\mathbf{1},\mathbf{2},3^+,4^+] &= g^2 m\hat{x}_{12} \times \frac{1}{s_{12}} \times \frac{[\hat{3}4]^3}{[4\hat{I}][\hat{I}\hat{3}]} \\ &= g^2 m^2 \frac{[4\hat{I}]}{\langle \hat{I}|p_1|4]} \times \frac{1}{s_{12}} \times \frac{[34]^3}{[4\hat{I}][\hat{I}\hat{3}]} \end{aligned} \tag{4.79}$$

and

$$-[3\hat{I}]\langle \hat{I}|p_1|4] \tag{4.80}$$

can be computed as following

$$\begin{aligned} -[3\hat{I}]\langle \hat{I}|p_1|4] &= -[3|(p_3+p_4)p_1|4] = [3|p_3p_1|4] - [3|p_4p_1|4] = -[3|p_4p_1|4] \\ &= -p_{4\mu}p_{1\nu}[3|(\bar{\sigma}^\mu)^{\dot{\alpha}\beta}(\sigma^\nu)_{\beta\dot{\gamma}}|4] \\ &= [3|p_1p_4|4] - 2p_1\cdot p_4[34] = -2p_1\cdot p_4[34] \end{aligned} \tag{4.81}$$

here we use the formula

$$(\sigma^\mu\bar{\sigma}^\nu + \sigma^\nu\bar{\sigma}^\mu)_\alpha{}^\beta = 2\eta^{\mu\nu}\delta_\alpha{}^\beta \tag{4.82}$$

and the term $2p_1\cdot p_4$ can be extracted from

$$(p_1+p_4)^2 = (p_2+p_3)^2 = s_{23} \tag{4.83}$$

The final result for this amplitude is

$$A[\mathbf{1},\mathbf{2},3^+,4^+] = \frac{[34]^3}{s_{34}(s_{23}-m^2)[43]} = m^2g^2\frac{[34]}{\langle 43\rangle(s_{23}-m^2)} \tag{4.84}$$

If we take the high energy limit so that the m can be chose to 0, then the amplitude becomes 0, which is consistent with our previous analysis.

For another helicity configuration, we can compute similarly

$$\begin{aligned} A[\mathbf{1},\mathbf{2},3^+,4^-] &= g^2 m\frac{1}{\hat{x}_{12}} \times \frac{1}{s_{12}} \times \frac{[\hat{I}\hat{3}]^3}{[\hat{3}4][4\hat{I}]} \\ &= g^2 m\frac{\langle \hat{I}|p_1|3]}{m[\hat{I}3]} \times \frac{[\hat{I}3]^3}{[34][4\hat{I}]} = g^2\frac{\langle \hat{I}|p_1|3][\hat{I}3]^2}{[34][4\hat{I}]s_{34}} \end{aligned} \tag{4.85}$$

aftering the similar computation, the final result can be obtained as

$$A[\mathbf{1},\mathbf{2},3^+,4^-] = g^2\frac{\langle 4|p_1|3]^2}{(s_{14}-m^2)s_{34}} \tag{4.86}$$

We can also take the high energy limit and check if it is consistent with our previous result.

Aftering some subtle computation, it can be proved that the amplitude can be written like

$$A = \frac{\langle 13\rangle[24][14]\langle 32\rangle}{[23]\langle 32\rangle[12]\langle 21\rangle} = \frac{\langle 14\rangle^2\langle 24\rangle^2}{\langle 12\rangle\langle 23\rangle\langle 34\rangle\langle 41\rangle} \tag{4.87}$$

which is perfectly math to the equation (4.16).(We neglect the negligible $\pm$ sign)

For the higher point case, in principle, there is no big difference from the computaion before, except the computaion for massive spinor-helicty variable.

5 Summary and Outlook

In this paper, we have explored scattering amplitudes within the framework of (De)constructed gauge theories, focusing specifically on the simplest 2-site model. Considering the well-known limitations of conventional Feynman diagram methods — particularly their complexity in handling the vast gauge redundancies and their failure to naturally exhibit hidden symmetries such as dual conformal invariance — modern amplitude techniques, such as the BCFW recursion relation, provide powerful alternatives. By leveraging complex momentum shifts, BCFW recursion effectively reduces higher-point scattering amplitudes to simpler lower-point amplitudes, offering substantial analytical and computational simplifications.

Our work applied the BCFW recursion relation alongside related modern amplitude methods, including color-ordering and spinor-helicity formalisms, to investigate tree-level scattering processes within this simplest two-site scenario. This model serves as an ideal testing ground due to its renormalizability and clear connection to higher-dimensional physics, specifically Kaluza-Klein (KK) modes emerging dynamically through dimensional deconstruction.

In addition to BCFW recursion, we have also incorporated the Cachazo-Svrček-Witten (CSW) expansion to compute next-to-maximally helicity-violating (NMHV) amplitudes. The CSW approach, based on the MHV vertex expansion, re-expresses amplitudes as connected diagrams built from on-shell MHV amplitudes and scalar propagators, offering an efficient alternative to traditional Feynman rules for nontrivial helicity sectors. Within our (De)constructed setup, the CSW framework enables a transparent decomposition of NMHV tree amplitudes and facilitates comparison with results obtained from BCFW, serving as a valuable complementary computational tool.

Looking forward, several promising directions arise naturally from our current study. Firstly, it is compelling to extend the two-site model analysis systematically to more intricate configurations, such as three-site or general n-site models. Increasing the number of sites allows for richer dynamical behavior and a more realistic representation of higher-dimensional gauge theories. Introducing massive scalar or gauge bosons into the model could further enhance realism, closely mimicking genuine KK spectra as encountered in phenomenological models of compactified extra dimensions.

Another intriguing avenue of future research involves incorporating gravity into this (De)constructed

framework. Developing a gravitational analogue through a similar deconstruction procedure, or applying the double-copy technique to our existing gauge-theoretic amplitudes, could yield novel gravitational amplitudes. Such gravitational models would enable the investigation of analogous cancellations observed in KK scattering, potentially offering insights into the intricate interplay between gauge theories and gravity.

Within the broader landscape of modern amplitude methods and higher-dimensional theories, various directions remain to be explored.

First, one natural extension is to apply on-shell techniques beyond the tree level. Loop amplitudes in gauge and gravity theories present formidable computational challenges when approached via traditional Feynman methods. However, modern on-shell approaches — such as generalized unitarity and integrand reduction — have proven to be powerful tools in reconstructing loop integrands from on-shell tree amplitudes [12]. Notably, certain extensions of BCFW recursion relations have also been proposed for one-loop amplitudes [13], where under carefully chosen complex momentum shifts, the integrands of loop-level diagrams can be constructed recursively using forward limits of tree amplitudes. These developments not only enable efficient computation but also reveal hidden structures in multi-loop amplitudes, such as iterative patterns and dual conformal invariance.

Secondly, the double-copy correspondence between gauge and gravity theories [14] opens a compelling avenue for constructing gravitational amplitudes from gauge-theoretic data. Applying double-copy techniques to (De)constructed gauge amplitudes may allow the generation of corresponding gravitational amplitudes, potentially illuminating novel relations between dimensional deconstruction and the emergence of semi-classical gravity.

Another important frontier is the celestial amplitude program [15], which reinterprets flat-space S-matrix elements as conformal correlators on the celestial sphere. Translating amplitudes from our (De)constructed framework into this basis may uncover new conformal structures and clarify connections to soft theorems and asymptotic symmetries, particularly in the context of dimensional emergence.

On-shell techniques have also begun to play a central role in understanding the classical dynamics of gravitating systems. Recent studies have demonstrated how scattering amplitudes can be used to compute classical observables, such as deflection angles and radiation profiles, in black hole encounters [16,17]. In particular, the use of amplitude-based methods to study black hole mergers and angular momentum transfer has gained traction [18]. Extending our methods to incorporate spinning particles or KK black hole analogs within (De)constructed frameworks may provide novel insights into the classical gravitational limit of higher-dimensional gauge systems.

Beyond computational techniques, recent advances have revealed that scattering amplitudes possess remarkably rich mathematical structures that transcend their Feynman diagram origins. The Cachazo-He-Yuan (CHY) formalism [19] [20] [21] reformulates tree-level amplitudes in a variety of theories — including gauge theory, gravity, and scalar theory — as contour integrals

over the moduli space of punctured Riemann spheres, localized on solutions to the so-called scattering equations. This approach unifies diverse theories into a single geometric framework and suggests a deep connection between worldsheet models and field theory amplitudes.

Building on such geometric insights, the notion of scattering forms [22] encodes amplitudes as differential forms on kinematic spaces or moduli spaces. These forms have logarithmic singularities only on physical poles, and their residues capture consistent factorization properties. Scattering forms provide a natural language for organizing amplitudes independently of specific Feynman representations, with close ties to positive geometry and canonical forms.

Most strikingly, in planar $\mathcal{N} = 4$ super Yang-Mills theory, the amplituhedron offers a geometric reformulation in which the integrand of scattering amplitudes is interpreted as the canonical form on a positive region of the Grassmannian. This picture bypasses locality and unitarity as input, instead deriving them from global geometric consistency. These developments highlight a profound shift: scattering amplitudes may ultimately be understood as emergent from geometry and combinatorics, rather than traditional Lagrangian dynamics.

Altogether, these directions — from higher-loop gauge and gravity amplitudes, to celestial reformulations, to classical black hole dynamics — point to a broad and rich landscape where modern amplitude techniques can deepen our understanding of spacetime, duality, and quantum gravity. The present work lays foundational steps toward the future goals within the context of (De)constructed quantum field theories or another different directions.

In conclusion, the results presented here set the foundation for future explorations into more complex (De)constructed models and their gravitational counterparts. These studies promise to deepen our understanding of amplitude structures, dimensional emergence, and the broader implications of gauge-gravity dualities.

A Conventions

In this paper we follow the mostly minus convention $(+,-,-,-)$, and an on-shell momentum satisfies $p^2 = m^2$. The sigma matrix are defined as

$$\sigma^\mu = (1, \vec{\sigma}), \qquad \bar{\sigma}^\mu = (1, -\vec{\sigma}). \tag{A.1}$$

The corressponding matrix form can be written like

$$p_{\alpha\dot{\alpha}} = p_\mu \sigma^\mu = \begin{pmatrix} E - p_3 & -p_1 + ip_2 \\ -p_1 - ip_2 & E + p_3 \end{pmatrix} \tag{A.2}$$

and

$$p^{\dot{\alpha}\alpha} = p_\mu \bar{\sigma}^\mu = \begin{pmatrix} E + p_3 & p_1 - ip_2 \\ p_1 + ip_2 & E - p_3 \end{pmatrix}. \tag{A.3}$$

Then it is easy to obtain their product

$$\begin{aligned} p_{\alpha\dot{\alpha}} \cdot p^{\dot{\alpha}\beta} &= \begin{pmatrix} E - p_3 & -p_1 + ip_2 \\ -p_1 - ip_2 & E + p_3 \end{pmatrix} \begin{pmatrix} E + p_3 & p_1 - ip_2 \\ p_1 + ip_2 & E - p_3 \end{pmatrix} \\ &= \begin{pmatrix} E - p^2 & 0 \\ 0 & E - p^2 \end{pmatrix} = m^2 \delta_\alpha^\beta, \end{aligned} \tag{A.4}$$

and

$$\det p_{\alpha\dot{\alpha}} = m^2. \tag{A.5}$$

We list the following properties for sigma matrix

$$(\bar{\sigma})^{\dot{\alpha}\alpha} = \varepsilon^{\alpha\beta}\varepsilon^{\dot{\alpha}\dot{\beta}}(\sigma)_{\beta\dot{\beta}} \tag{A.6}$$

$$(\sigma)_{\alpha\dot{\alpha}}(\sigma)_{\beta\dot{\beta}} = 2\varepsilon_{\alpha\beta}\varepsilon_{\dot{\alpha}\dot{\beta}} \tag{A.7}$$

$$(\sigma^\mu\bar{\sigma}^\nu + \sigma^\nu\bar{\sigma}^\mu)_\alpha{}^\beta = 2\eta^{\mu\nu}\delta_\alpha{}^\beta \tag{A.8}$$

$$\mathrm{Tr}(\sigma^\mu\bar{\sigma}^\nu) = \mathrm{Tr}(\bar{\sigma}^\mu\sigma^\nu) = 2\eta^{\mu\nu} \tag{A.9}$$

The Gamma matrices are defined like

$$\gamma^\mu = \begin{pmatrix} 0 & (\sigma)_{\alpha\dot{\alpha}} \\ (\bar{\sigma})^{\dot{\alpha}\alpha} & 0 \end{pmatrix}, \qquad \{\gamma^\mu, \gamma^\nu\} = 2\eta^{\mu\nu} \tag{A.10}$$

The $\mathrm{SL}(2,\mathbb{C})$ and $\mathrm{SU}_L(2)$ indices are raised and lowered as

$$\psi_\alpha = \psi^\beta \varepsilon_{\alpha\beta}, \quad \psi^\alpha = \varepsilon^{\alpha\beta}\psi_\beta, \quad \varepsilon^{\alpha\beta}\varepsilon_{\beta\gamma} = \delta^\alpha_\gamma \tag{A.11}$$

where the ψ refers to a Weyl spinor belonging to $SU(2)_L$ representation (left-handed spinor),

and it is same for $SU(2)_R$ (right-handed spinor). We use $\varepsilon_{\alpha\beta} = -\varepsilon^{\alpha\beta} = \begin{pmatrix} 0 & -1 \\ 1 & 0 \end{pmatrix}$, the anti-symmetric tensor, to rasie and lower the index. More general for eqution (A.4), two different spinor contraction can be converted to vector contraction following

$$p_1^{\alpha\dot{\alpha}} p_{2\alpha\dot{\alpha}} = 2p_1^{\mu} p_{2\mu}, \tag{A.12}$$

where we use the formula (A.9) and hence for massive momenta, $p^{\alpha\dot{\alpha}} p_{\alpha\dot{\alpha}} = 2m^2$, it can also be noticed from (A.4). The vector indices are converted to spinorial ones for massive case as:

$$\gamma^{\mu} = \begin{pmatrix} 0 & \sigma^{\mu}_{\alpha\dot{\beta}} \\ \bar{\sigma}^{\mu\dot{\alpha}\beta} & 0 \end{pmatrix} \quad \rightarrow \quad (\not{p} + m) = \begin{pmatrix} m\delta^{\beta}_{\alpha} & p_{\alpha\dot{\beta}} \\ p^{\dot{\alpha}\beta} & m\delta^{\dot{\alpha}}_{\dot{\beta}} \end{pmatrix} \tag{A.13}$$

For convenience, we also collect some useful identities for spinor-helicity variable:

$$\begin{gathered}
[p|_{\dot{\alpha}} = \varepsilon_{\dot{\alpha}\dot{\beta}} |p]^{\dot{\beta}}, \qquad \langle p|^{\alpha} = \varepsilon^{\alpha\beta} |p\rangle_{\beta}, \\
|p]^{\dot{\alpha}} = \varepsilon^{\dot{\alpha}\dot{\beta}} [p|_{\dot{\beta}}, \qquad |p\rangle_{\alpha} = \varepsilon^{\alpha\beta} \langle p|_{\beta}, \\
p_{\alpha\dot{\alpha}} = |p\rangle_{\alpha} [p|_{\dot{\alpha}}, \qquad p^{\dot{\alpha}\alpha} = |p]^{\dot{\alpha}} \langle p|^{\alpha}, \\
\not{p} = |p\rangle_{\alpha} [p|_{\dot{\alpha}} + |p]^{\dot{\alpha}} \langle p|^{\alpha}, \\
\langle pq\rangle = \langle p|^{\alpha} |q\rangle_{\alpha}, \qquad [pq] = [p|_{\dot{\alpha}} |q]^{\dot{\alpha}}, \\
\langle pq\rangle [qp] = 2p \cdot q = (p+q)^2 \quad , \\
\text{(the last equality only holds for massless particle)} \\
[k|\sigma^{\mu}|p\rangle] = \langle p|\sigma^{\mu}|k], \qquad [k|\sigma^{\mu}|p\rangle] = \langle k|\sigma^{\mu}|p] \text{ (for real moemnta)}, \\
\langle p|P|k] = \langle p|^{\alpha} P_{\alpha\dot{\alpha}} |k]^{\dot{\alpha}}, \qquad \langle p|y_1 y_2|k\rangle = \langle p|^{\alpha} y_{1\alpha\dot{\alpha}} y_2^{\dot{\alpha}\beta} |p\rangle_{\beta}, \\
\langle p|q|k] = \langle pq\rangle [qk], \qquad \langle 1|\gamma^{\mu}|2] \langle 3|\gamma_{\mu}|4] = 2\langle 13\rangle [24].
\end{gathered} \tag{A.14}$$

The analytic continuation are choosen like

$$|-p\rangle = -|p\rangle, \qquad |-p] = +|p]. \tag{A.15}$$

The angle spinor and square spinor are related by complex conjugation:

$$[p|_{\dot{\alpha}} = (|p\rangle_{\alpha})^*, \qquad \langle p|^{\alpha} = (|p]^{\dot{\alpha}})^* \tag{A.16}$$

for real momenta p.

B Polarization Vectors

In quantum field theory, the quantities computed directly from Feynman diagrams, such as $M^\mu(p,\cdots)$, are Lorentz tensors. However, these objects by themselves do not possess the correct transformation properties to be regarded as physical scattering amplitudes. In particular, they fail to transform appropriately under the little group associated with massless particles.

To bridge this gap, we introduce *polarization vectors* $\epsilon^\mu_\sigma(p)$, whose role is to carry the correct little group behavior. These vectors transform under Lorentz transformations as

$$\epsilon^\mu_\sigma(\Lambda p) = \Lambda^\mu{}_\nu\, \epsilon^\nu_{\sigma'}(p)\, D_{\sigma'\sigma}(W),$$

where $D(W)$ is the representation of the little group element W associated with the Lorentz transformation Λ. In this way, the contraction

$$\epsilon^\mu_\sigma(p)\, M_\mu(p,\cdots)$$

transforms correctly as a scalar (or spinor/tensor) amplitude under both Lorentz and little group actions.

It is important to emphasize that in modern amplitude formulations—particularly those employing spinor-helicity variables or on-shell recursion relations—polarization vectors are not fundamental ingredients. Rather, they serve as auxiliary tools to extract the physical content from intermediate Feynman tensor structures. The true scattering amplitude is inherently a little group covariant object, and in spinor-helicity language, this structure is built directly into the helicity-spinor formalism. In fact, as demonstrated in the main text, one can carry out the entire computation without ever introducing polarization vectors. Nevertheless, in certain contexts, particularly when comparing with Feynman diagrammatic results or for pedagogical clarity, their use remains convenient and insightful.

The external line rule for an outgoing massless spin-1 vector boson is implemented by contracting the amplitude with its polarization vector. In the spinor-helicity formalism, the polarization vectors can be expressed as:

$$\epsilon^\mu_-(p;q) = -\frac{\langle p|\gamma^\mu|q]}{\sqrt{2}[q\,p]}, \qquad \epsilon^\mu_+(p;q) = -\frac{\langle q|\gamma^\mu|p]}{\sqrt{2}\langle q\,p\rangle}, \tag{B.1}$$

where $q \neq p$ is an arbitrary reference spinor. The choice of reference spinor encodes gauge redundancy, and the physical amplitude remains unchanged under shifts of the form

$$\epsilon^\mu_\pm(p) \to \epsilon^\mu_\pm(p) + C\, p^\mu.$$

The Weyl equation for massless spinors ensures that $p_\mu \epsilon^\mu_\pm(p) = 0$. In practice, the polariza-

tion vectors are often written in a spinor outer-product form:

$$\not{\epsilon}_-(p;q) = \frac{\sqrt{2}}{[q\,p]}\left(|p][q| + |q][p|\right), \qquad \not{\epsilon}_+(p;q) = \frac{\sqrt{2}}{\langle q\,p\rangle}\left(|p\rangle\langle q| + |q\rangle\langle p|\right). \tag{B.2}$$

This freedom in choosing the reference spinor reflects gauge invariance. It does not affect on-shell amplitudes, due to the Ward identity $p_\mu A_n^\mu = 0$. For each external gluon (or massless vector), one can freely choose a $q_i \neq p_i$ for defining its polarization. However, consistency requires that the same q_i be used across all diagrams within a given process. Importantly, the full physical amplitude remains independent of the reference spinors after summing over diagrams.

We consider a massless four-momentum given by

$$p^\mu = (E,\ E\sin\theta\cos\phi,\ E\sin\theta\sin\phi,\ E\cos\theta)\,,$$

which corresponds to a particle moving at an angle θ from the z-axis and azimuthal angle ϕ in spherical coordinates. In Exercise 2.1, the spinor-helicity variables $|p]$ and $[p|$ associated with this momentum were constructed explicitly.

In this context, we now relate the spinor-helicity polarization vectors from the previous section to the conventional polarization vectors defined in coordinate space. The standard helicity eigenstate vectors take the form:

$$\tilde{\epsilon}_\pm^\mu(p) = \pm\frac{e^{\mp i\phi}}{\sqrt{2}}\left(0,\ \cos\theta\cos\phi \pm i\sin\phi,\ \cos\theta\sin\phi \mp i\cos\phi,\ -\sin\theta\right).$$

These expressions clearly show the transverse nature of the polarization with respect to the direction of motion. In the special case where $\theta = \phi = 0$, i.e., the particle moves along the z-axis, the polarization vectors reduce to

$$\tilde{\epsilon}_\pm^\mu(p) = \pm\frac{1}{\sqrt{2}}(0,\ 1,\ \mp i,\ 0),$$

which correspond to circular polarization in the xy-plane.

Example. Consider the 3-point QED amplitude $A_3(f^{h_1}\bar{f}^{h_2}\gamma^{h_3})$, where $f = e^-$ and $\bar{f} = e^+$ denote the outgoing massless electron and positron, respectively. Let us take the helicities to be $h_1 = -\frac{1}{2}$, $h_2 = +\frac{1}{2}$, and $h_3 = -1$. The corresponding Feynman amplitude is given by:

$$iA_3(f^-\bar{f}^+\gamma^-) = \bar{u}_-(p_1)\,(ie\gamma_\mu)\,v_+(p_2)\,\epsilon_-^\mu(p_3;q)$$

Using spinor-helicity variables, this becomes:

$$= ie\langle 1|\gamma_\mu|2]\frac{[3|\gamma^\mu|q]}{\sqrt{2}[3q]} = \sqrt{2}ie\frac{\langle 13\rangle[2q]}{[3q]}$$

where we have applied the Fierz identity in the last step to simplify the spinor contractions.

Hence, the amplitude reduces to:

$$A_3(f^-\bar{f}^+\gamma^-) = \tilde{e}\,\frac{\langle 13\rangle[2q]}{[3q]}$$

with the shorthand coupling $\tilde{e} \equiv \sqrt{2}e$ absorbing the normalization factor into the definition of the coupling constant. This is the reason why we use $\tilde{e}$ instead of e in the main context.

Without doubt, the physical amplitude should not depend on arbitrary reference spinor q. To eliminate the reference spinor $|q]$ appearing in the denominator, we first multiply the amplitude by the identity factor $\langle 12\rangle/\langle 12\rangle$. This transforms the numerator as follows:

$$\langle 13\rangle\langle 12\rangle[2q].$$

Next, using momentum conservation $p_2 = -p_1 - p_3$ and the massless Dirac equation $\langle 1|p_2 = -\langle 1|(p_1 + p_3)$, we compute:

$$\langle 12\rangle[2q] = -\langle 1|p_2|q] = \langle 1|(p_1 + p_3)|q] = \langle 13|q] = \langle 13\rangle[3q].$$

Thus, the numerator becomes $\langle 13\rangle^2[3q]$, and the factor of $[3q]$ cancels with the same term in the denominator of the original expression.

We are therefore left with a compact expression:

$$A_3(f^-\bar{f}^+\gamma^-) = \tilde{e}\,\frac{\langle 13\rangle^2}{\langle 12\rangle},$$

which is manifestly independent of the arbitrary reference spinor q.

References

[1] Henriette Elvang and Yu-tin Huang. Scattering Amplitudes. 8 2013.

[2] Vittorio Del Duca, Lance J. Dixon, and Fabio Maltoni. New color decompositions for gauge amplitudes at tree and loop level. *Nucl. Phys. B*, 571:51–70, 2000.

[3] Nima Arkani-Hamed, Andrew G. Cohen, and Howard Georgi. (De)constructing dimensions. *Phys. Rev. Lett.*, 86:4757–4761, 2001.

[4] Bo Feng and Mingxing Luo. An Introduction to On-shell Recursion Relations. *Front. Phys. (Beijing)*, 7:533–575, 2012.

[5] Andrew Hodges. Eliminating spurious poles from gauge-theoretic amplitudes. *JHEP*, 05:135, 2013.

[6] Nima Arkani-Hamed and Jaroslav Trnka. The Amplituhedron. *JHEP*, 10:030, 2014.

[7] Timothy Cohen, Henriette Elvang, and Michael Kiermaier. On-shell constructibility of tree amplitudes in general field theories. *JHEP*, 04:053, 2011.

[8] Henriette Elvang, Daniel Z. Freedman, and Michael Kiermaier. Proof of the MHV vertex expansion for all tree amplitudes in N=4 SYM theory. *JHEP*, 06:068, 2009.

[9] Freddy Cachazo, Peter Svrcek, and Edward Witten. MHV vertices and tree amplitudes in gauge theory. *JHEP*, 09:006, 2004.

[10] Sourav Ballav and Arkajyoti Manna. Recursion relations for scattering amplitudes with massive particles. *JHEP*, 03:295, 2021.

[11] Nima Arkani-Hamed, Tzu-Chen Huang, and Yu-tin Huang. Scattering amplitudes for all masses and spins. *JHEP*, 11:070, 2021.

[12] Z. Bern, L. J. Dixon, D. C. Dunbar, and D. A. Kosower. Fusing gauge theory tree amplitudes into loop amplitudes. *Nucl. Phys. B*, 435:59–101, 1995.

[13] Savan Kharel and George Siopsis. Gauge theory one-loop amplitudes and the BCFW recursion relations. *Phys. Rev. D*, 86:025004, 2012.

[14] Z. Bern, J. J. Carrasco, and H. Johansson. Perturbative Quantum Gravity as a Double Copy of Gauge Theory. *Phys. Rev. Lett.*, 105:061602, 2010.

[15] Sabrina Pasterski, Shu-Heng Shao, and Andrew Strominger. Gluon Amplitudes as 2D Conformal Correlators. *Phys. Rev. D*, 96(8):085006, 2017.

[16] Alfredo Guevara, Ben Maybee, and Justin Vines. Scattering of Spinning Black Holes from Exponentiated Soft Factors. *JHEP*, 12:027, 2019.

[17] Duff Neill and Ira Z. Rothstein. Classical Space-Times from the S Matrix. *Nucl. Phys. B*, 877:177–189, 2013.

[18] Katsuki Aoki, Andrea Cristofoli, and Yu-tin Huang. On-shell approach to black hole mergers. *JHEP*, 01:066, 2025.

[19] Freddy Cachazo, Song He, and Ellis Ye Yuan. Scattering equations and Kawai-Lewellen-Tye orthogonality. *Phys. Rev. D*, 90(6):065001, 2014.

[20] Freddy Cachazo, Song He, and Ellis Ye Yuan. Scattering of Massless Particles in Arbitrary Dimensions. *Phys. Rev. Lett.*, 113(17):171601, 2014.

[21] Freddy Cachazo, Song He, and Ellis Ye Yuan. Scattering of Massless Particles: Scalars, Gluons and Gravitons. *JHEP*, 07:033, 2014.

[22] Nima Arkani-Hamed, Yuntao Bai, Song He, and Gongwang Yan. Scattering Forms and the Positive Geometry of Kinematics, Color and the Worldsheet. *JHEP*, 05:096, 2018.